Chapter 2
Multi-Effect-Coupling pH-Stimulus (MECpH) Model for pH-Sensitive Hydrogel

2.1 Introduction

In general, the degree of swelling/shrinking of a smart hydrogel is dependent upon many effects, such as the ionizable group and polymeric network structure of the hydrogel and the characteristics of environmental solutions including the composition, pH and temperature, in which there are different interactions between mechanical, chemical and electrical fields.

In this chapter, a multiphysics model is developed for simulation of the swelling/deswelling behaviour of the hydrogel responsive to surrounding pH when the hydrogel is immersed in the buffered solution, called the multi-effect-coupling pH- stimulus (MECpH) model. The model is based on Poisson–Nernst–Planck (PNP) formulation and derived in combination with the species diffusion, pendent ionizable group dissociation reaction and electric potential effect for the distributive profiles of ionic concentrations and electric potential within both the hydrogel and bathing solution domains in response to the change in pH of surrounding solution. The PNP equations are coupled with nonlinear mechanical equilibrium governing equation for analysis of large deformation of the pH-sensitive hydrogel. The MECpH model is validated by comparison between the simulation results and published experiment data available in the literature. It is followed by comprehensive parameter studies for the influences of hydrogel material properties and environmental solutions on the responsive performance of the pH-sensitive hydrogel when placed in the buffered solution.

2.2 Development of the MECpH Model

Extensive search of literature reveals that most of the theoretical models are either oversimplified to limit applicability or too complex to account flexibly for significant parameters requested by experiments. Therefore, the objective of this section is to formulate a theoretical model with clear fundamental, very robustness and possible extension for a wide range of applications. This is a multiphysics model and termed the multi-effect-coupling pH-stimulus (MECpH) model. It is developed

H. Li, *Smart Hydrogel Modelling*, DOI 10.1007/978-3-642-02368-2_2,

mathematically to simulate the behaviour of the pH-sensitive hydrogels in response to infinitesimal changes in environmental conditions.

Basically the Nernst–Planck flux system is employed to describe the mechanism of transports of diffusive species in a membrane. It is known that the Nernst–Planck system is insufficient as it only includes the effects of the gradients of species concentration and electrical potential. Over the past decades, many researchers chose the computational models simplified by assuming the electroneutrality condition or constant field. These are the two widely used assumptions and also the two limited cases of certain dimensionless parameters associated with the ratio of the Debye length to membrane thickness. Therefore, the Nernst–Planck system is not sufficiently accurate for some electrolytic solutions, especially for the presently considered hydrogels with fixed charge groups, which are often used for description of biological systems like thin membranes. A more rigorous model is necessarily developed to include the variation of the electric potential based on the spatial distribution of the electric charges, where the relationship between the electrical potential and the various ionic fluxes is required by coupling with the Poisson equation, which forms the PNP system. According to this system, the drift of an ionic species strongly influences those of all other ions dissolved in the electrolytic solutions. Further, the model couples the mechanical equilibrium equation by a finite deformation formulation with the PNP equations to simulate the large deformation of hydrogels.

One of the important contributions in development of the MECpH model is to incorporate a relation between the diffusive hydrogen ions and the fixed charge attached onto the polymeric chain network of the hydrogels, which is based on the Langmuir adsorption isotherm with consideration of the hydrogen ion bound by the fixed charge groups.

The MECpH model simulating the pH-responsive hydrogels is able to provide the concentration profiles of all diffusive ionic species, the electric potential distribution in both the hydrogel and bathing solution domains as well as the mechanical deformation of the hydrogels swollen in the surrounding solutions with various environmental conditions.

2.2.1 Electrochemical Formulation

As well known, there are several possible approaches to simulating the ion permeation at atomistic level, including all-atom molecular dynamics, Brownian dynamics and Monte Carlo simulations. However, the continuum formulations are still very valuable for highlighting fundamental principles in a particularly clear fashion, even though they often overlook the fine details of atomic-level reality that becomes significant at microscopic level. Further, when we deal with millions of ions interacting each other and with polymeric chains, it is much more practical in a sense to investigate the ion transport within the hydrogel in a continuum manner. In particular, the macroscopic continuum electrostatic simulation is based

on the capability of choosing infinitesimal element volume of interest but large enough to cover sufficient number of charge groups, such that meaningful volume charge density can be characterized in a continuous sense and thus it can illustrate fundamental principles in a comprehensible way (Woodson and Melcher, 1968; Grodzinsky, 1974).

For the continuum theories developed for electrodiffusion modelling, Poisson–Nernst–Planck (PNP) equation has been applied successfully for describing the ion transportation phenomena in the polyelectrolyte gel (Gulch et al., 2000; Wallmersperger et al., 2001), the ion exchange or biological membrane (Helfferich, 1962; Carnay and Tasaki, 1971; Sjodin, 1971; Rubinstein, 1990), the biological ion channel (Kurnikova et al., 1999; Syganow and von Kitzin, 1999; Gillespie and Eisenberg, 2001, 2002; Roux et al., 2004), semiconductor (Selberherr, 1984), soil or clay (Samson et al., 1999; Samson and Marchand, 1999) and other porous media (MacGillivray, 1968; MacGillivray and Hare, 1969; Kato, 1995).

In the PNP system, the electric field is calculated self-consistently by the average ionic charge density. The ion–ion interactions are thus incorporated approximately at a mean field level (Eisenberg, 1999), namely it is the possible best way to find out the chemical properties of porous media by making them as small as possible for further understanding with mean electrostatic field. If the phenomena observed cannot be described well by the mean field, we then turn to chemically specific explanations for seeking out appropriate tools, for example, Langevin or molecular dynamics. This strategy will be followed up in the following sections for analysis of electrodiffusion within the hydrogel.

2.2.1.1 Ionic Flux

Hydrogel is generally composed of crosslinked polymer network matrix binding the fixed charge groups, where there exist mobile co-ions and counterions surrounding the mesh network within the interstitial fluid. The flow of fluxes rises generally due to the gradients of ionic concentration, electrical potential, chemical potential or pressure. As well known, the Nernst–Planck equation can characterize the ionic fluxes in the hydrogel in terms of the gradients of the ionic concentration, electrical potential and pressure. By the law of mass conservation, the ionic fluxes and species concentrations can be formulated in the form of macroscopic continuum. Therefore, the Nernst–Planck equations for ion transportation phenomena in the system can be written as follows for the flux of ionic species k (Teorell, 1953; Dresner, 1972):

$$\begin{aligned}\mathbf{J}_k &= -[[D_k]_i \mathbf{grad}(c_k) + F\mu_k z_k c_k \mathbf{grad}(\psi) + [D_k]_i c_k \mathbf{grad}(\ln \gamma_k)] + c_k \mathbf{U}_i \\ &= -[D_k]_i [\mathbf{grad}(c_k) + \tfrac{F}{RT} z_k c_k \mathbf{grad}(\psi) + c_k \mathbf{grad}(\ln \gamma_k)] + c_k \mathbf{U}_i \qquad (2.1) \\ &\qquad (k = 1,2,3,...,N_{\text{ion}})\end{aligned}$$

where $\boldsymbol{J}_k$ (mM/s) is the flux of the kth species and N_{ion} is the number of total species in the system. D_k (m^2/s) is the diffusivity tensor of the kth species, i is the direction of flux flow. c_k (mM) and z_k are the concentration and valence number of the kth diffusive ionic species, respectively. μ_k (m**.**mol/s) is the mobility of the kth ion species, ψ (V) is the electrostatic potential, γ_k is the chemical activity coefficient of the kth species and $\boldsymbol{U}_i$ (m/s) is the fluid velocity relative to the polymer matrix network. F, R and T are the Faraday's constant (9.6487×10^4 C/mol), universal gas constant (8.314 J/mol·K) and absolute temperature (K), respectively.

The first term on the right-hand side of Eq. (2.1) represents the diffusive flux due to the gradient of concentration in the domain. This term is identical with the Fick's first law of diffusion equation. The spatial distribution of concentration $c_k(\mathbf{x})$ could be a linearly continuous gradient or becomes more complicated with irregular concentration pattern (Katchalsky and Curran, 1965).

The second term represents the migration flux arising from the gradient of the electrical potential. It is applicable when electrostatic force exists with or without the externally applied electric voltage. The electric potential could vary linearly across the domain that is so-called constant field condition. The distribution of the electric potential could also be governed by the Poisson equation. Therefore, the profiles of species concentration are influenced by the bulk concentration and the distributive electric field (Helfferich, 1962).

The third term is associated with the chemical activity coefficient of ion species in non-ideal electrolyte solution. There are several semi-empirical formulae developed for computing the chemical activity coefficient. However, the Debye–Huckel model may be one of the most popular mathematical descriptions to determine the activity coefficient. In addition, it should be noted that the rate of the ionic diffusion is much faster than the kinetics of chemical activity if an external electric field is applied. Therefore, the contribution of the chemical activity coefficient is very small relatively and thus negligible. More studies of the effect of the chemical activity coefficient can be found (Bockris and Reddy-Amulya, 1998; Samson et al., 1999).

The fourth term refers to the convective flux resulting from the fluid velocity due to the electro-osmosis solvent flow. The convection flux is described relatively to some reference velocities, which may be the average velocities of mass, molar, volume or solvent (Cussler, 1997). However, in the present analysis for the case of an unstirred solution in vibration-free experimental device, this term can be neglected for simplicity because the bulk fluid flow or hydrodynamic velocity vanishes and subsequently the convective flux becomes negligible (Marchiano and Arvia, 1983).

According to the law of mass conservation, the change in the amount of the kth species contained in the volume with respect to time t is characterized by the difference between the fluxes entering and leaving the reference volume (Yeager et al., 1983). Therefore, the continuity equation of the kth diffusive species is derived as follows:

$$\frac{\partial c_k}{\partial t} + \mathrm{div}(\mathbf{J}_k) = 0$$

or

$$\frac{\partial c_k}{\partial t} + \mathrm{div}\{-[[D_k]_i \mathbf{grad}(c_k) + F\mu_k z_k c_k \mathbf{grad}(\psi) + [D_k]_i c_k \mathbf{grad}(\ln \gamma_k)] + c_k \mathbf{U}_i\} = 0$$

or

$$\frac{\partial c_k}{\partial t} + \mathrm{div}\left\{ -[D_k]_i \left[\mathbf{grad}(c_k) + \frac{F}{RT} z_k c_k \mathbf{grad}(\psi) + c_k \mathbf{grad}(\ln \gamma_k) \right] + c_k \mathbf{U}_i \right\} = 0$$

$(k = 1,2,3,\ldots,N_{\mathrm{ion}})$ (2.2)

The above equation, often known as the Nernst–Planck equation, involves the unknown mobility μ_k which can be determined by the Nernst–Einstein relationship as follows:

$$\mu_k = \frac{D_k}{RT} \tag{2.3}$$

Usually the diffusion coefficient of solute in hydrogels is dependent on many effects, including the size of the solute molecule relative to the structure and pore size of the polymeric gel, the polymer chain mobility and the water content. Peppeas et al. (2000) have put these effects into a general form as follows:

$$\frac{D_k}{D_0} = f(r_k, \phi_s, \xi) \tag{2.4}$$

where D_k is the effective diffusion coefficient and D_0 is the corresponding diffusion coefficient of solute in pure solvent. r_k is the radius of the diffusive molecule, ϕ_s is the volume fraction of polymer network in the hydrogel and ξ is network mesh size. The reviews of various theoretical models were made by Muhr and Blanshard (1982) and Amsden (1998). However, it is also shown from experimentally measured data that the diffusion coefficient is almost constant with swelling of the hydrogel but it is time dependent (Gehrke and Cussler, 1989).

2.2.1.2 Electrical Potential

For the distributive pattern of electrical potential, there are a few possible ways to describe its distribution, such as the electroneutrality or null current assumption (Hwang, and Helfferich, 1987; Doi et al., 1992; Samson and Marchand, 1999) or the constant field assumption (Malmivuo and Plonsey, 1995; Gillespie and Eisenberg, 2002). However, the Poisson equation is a more rigorous formulation (Helfferich, 1962; MacGillivray, 1968; MacGillivray and Hare, 1969). Each of them will be evaluated, and it will be shown that the constant field and electroneutrality assumptions are indeed the two limited cases of the Poisson equation.

Constant Field

The assumption of constant field in fact implies that the electric potential varies linearly across the system. In other words, the gradient of electric potential in the hydrogel is constant. This assumption was introduced first for analysis of ion transport through biological membrane (Goldman, 1943; Hodgkin and Katz, 1949), where the membrane is assumed to be uniform, planar and infinite in its lateral extent. Hence, the potential field ψ and ionic concentration c within the membrane are functions of x only. One can thus have

$$\frac{\partial^2 \psi}{\partial x^2} = 0 \tag{2.5}$$

If the membrane has a thickness of h

$$\frac{d\psi}{dx} \approx \frac{\psi(h) - \psi(0)}{h} = \frac{V_m}{h} \tag{2.6}$$

where V_m is the transmembrane voltage.

Constant Current

Following the assumptions of the electroneutrality conserved everywhere and the global flow of all ions across the boundary yielding null current, the additional conditions to support the Nernst–Planck flux equation (2.2) are summarized as follows:

Electroneutrality in the interior hydrogel:

$$\sum_k z_k c_k + z_f c_f = 0 \tag{2.7}$$

Electroneutrality in the exterior bathing solution:

$$\sum_k z_k c_k = 0 \tag{2.8}$$

Null current:

$$\sum_k z_k \boldsymbol{J}_k = 0 \tag{2.9}$$

where c_k is the concentration of the kth ion species either inside or surrounding the hydrogel. c_f is the density of the fixed charge group within the hydrogel.

Poisson Equation

The Poisson equation is a more rigorous approach to characterize the spatial distribution of the electric potential in the domain. In the studies of membrane immersed in physiological electrolytic environment, it is commonly accepted that the electric field near or in the membrane is of primary importance and the magnetic and electromagnetic phenomena inherently play a second role (Goldman, 1971). Therefore, the formulation can be limited to the case of an electrostatic field for deriving the Poisson equation (Panofsky and Phillips, 1964). The basic equations describing the electrostatic field are given as follows:

$$\nabla \times \mathbf{E}_{el} = 0 \tag{2.10}$$

$$\nabla \cdot \mathbf{E}_{el} = \frac{\rho_{el}}{\varepsilon_0} \tag{2.11}$$

$$\mathbf{E}_{el} \equiv -\nabla\psi \tag{2.12}$$

where $\mathbf{E}_{el}$ is the macroscopic average electric field acting on the charges within the medium, ψ is the electric potential, ρ_{el} (C/cm^3) is the charge density in an average volume and ϵ_0 the vacuum permittivity of free space or dielectric constant (8.85418×10^{-12}C^2/Nm^2). The above three equations are termed Maxwell's equations and Eq. (2.12) results from Eq. (2.11), which means that the electrostatic field is irrotational (Panofsky and Phillips, 1964).

Let us define the divergence of tensor $\mathbf{E}_{el}$ in terms of a scalar potential ψ as follows:

$$\nabla \cdot \mathbf{E}_{el} = \nabla \cdot (-\nabla\psi) = -\nabla^2\psi \tag{2.13}$$

By Maxwell's equation (2.11), Gauss's law proves

$$\nabla^2\psi = -\frac{\rho_{el}}{\varepsilon_0} \tag{2.14}$$

Equation (2.14) is known as the Poisson equation. If the condition of zero charge, $\rho_{el} = 0$, is imposed, the Poisson equation is reduced to Laplace equation as follows:

$$\nabla^2\psi = 0 \tag{2.15}$$

Equation (2.15) is equivalent to Eq. (2.5), which results from the constant field assumption.

From Maxwell's equation (2.10)

$$\nabla \times \mathbf{E}_{el} = \nabla \times (-\nabla\psi) = 0 \tag{2.16}$$

The curl law of Eq. (2.10) makes sure that $\mathbf{E}_{el}$ could be represented by the gradient of a scalar. Hence, $\nabla \times \mathbf{E}_{el} = 0$ permits $\mathbf{E}_{el} \equiv -\nabla\psi$; in return, $\mathbf{E}_{el} \equiv -\nabla\psi$

guarantees $\nabla \times \mathbf{E}_{el} = 0$. In addition, it is known that ψ can be determined just by a differential equation, i.e. Poisson equation, because ψ is a scalar. However, the determination of tensor $\mathbf{E}_{el}$ requires the presence of both the divergence and curl conditions.

In fact, the source of electric field is often separated into two types, the truly free charge ρ_{el} and the polarization or bound charge ρ_P, because of the material medium. Therefore, the Poisson equation (2.14) becomes

$$\nabla^2 \psi = -\nabla \cdot \mathbf{E}_{el} = -\left(\frac{\rho_{el} + \rho_P}{\varepsilon_0}\right) \tag{2.17}$$

Further, it is more convenient to express ρ_P in terms of the divergence of the polarization $\mathbf{P}_{el}$:

$$-\nabla \cdot \left(\mathbf{E}_{el} + \frac{\mathbf{P}_{el}}{\varepsilon_0}\right) = -\frac{\rho_{el}}{\varepsilon_0} \tag{2.18}$$

Therefore, we can define the electric displacement $\mathbf{D}_{el}$ (C/m^2) as

$$\mathbf{D}_{el} = \varepsilon_0 \mathbf{E}_{el} + \mathbf{P}_{el} \tag{2.19}$$

and subsequently Gauss's law in terms of $\mathbf{D}_{el}$ is given as

$$\nabla \cdot \mathbf{D}_{el} = \rho_{el} \tag{2.20}$$

For the medium with linear dielectrics, the polarization is $\mathbf{P}_{el} = \varepsilon_0(\varepsilon - 1)\mathbf{E}_{el}$ and Eq. (2.19) becomes

$$\mathbf{D}_{el} = \varepsilon \varepsilon_0 \mathbf{E}_{el} \tag{2.21}$$

where ε is the relative dielectric constant of the surrounding medium. After rearrangement, the general Poisson equation is obtained as

$$\nabla^2 \psi = -\frac{\rho_{el}}{\varepsilon \varepsilon_0} \tag{2.22}$$

The truly free charge ρ_{el} is a function of all ionic concentrations in solution and it is calculated by

$$\rho_{el} = F\left(\sum_k z_k c_k + z_f c_f\right) \tag{2.23}$$

Therefore, the Poisson equation can be finally written in the following form to characterize the spatial distribution of the electric potential in domain:

$$\nabla^2 \psi = -\frac{F}{\varepsilon \varepsilon_0}\left(\sum_k z_k c_k + z_f c_f\right) \tag{2.24}$$

The Poisson equation embodies a mean field of electric potential ψ, which approximates the interactions of ion–ion and ion with the fixed charge. It is noted that ψ is generally the sum of the externally applied potential and diffusion potential. This is a mean field potential, instead of instantaneous potential, and it serves as the mean electrical driving force on the ions, about which the instantaneous potential fluctuates (Cooper et al., 1985). It is observed that the constant field and electroneutrality assumptions are in fact the special cases of the Poisson equation. The constant field assumption is valid for low ionic concentrations, while the electroneutrality with null current assumption is applicable only if the ionic concentrations are high (MacGillivray, 1968; MacGillivray and Hare, 1969).

If one needs to add the screening condition at microscopic level, the Poisson equation (2.22) can be extended conveniently to Poisson–Boltzmann equation, which is a mean field approximation approach including the electrostatic system through the Poisson equation and the effect of entropy, because of the mobility of the counterions through the Boltzmann distribution of statistical mechanics. Then, if $\rho(\mathbf{x}) = \rho_{\text{fixed}}(\mathbf{x}) + \rho_{\text{mobile}}(\mathbf{x})$ is the charge density as the function of coordinate position, the Poisson equation becomes

$$\nabla^2\psi = -\frac{\rho_{\text{fixed}}(\mathbf{x}) + \rho_{\text{mobile}}(\mathbf{x})}{\varepsilon\varepsilon_0} \tag{2.25}$$

According to the statistical mechanics, if only an ion species with charge q is mobile, the relative probability of finding an ion at position $\mathbf{x}$ is given by the Boltzmann expression, $\exp(-q\psi(\mathbf{x})/k_BT)$, where k_B is Boltzmann's constant (1.3807×10^{-23}J/K) and T is the absolute temperature. The profile of charge density is then expressed by

$$\rho_{\text{mobile}}(\mathbf{x}) = qc_0 \exp(-q\psi(\mathbf{x})/k_BT) \tag{2.26}$$

where c_0 is the ion density for the ions per volume at a point where the electrostatic potential vanishes. The Poisson equation (2.22) is thus extended into the Poisson–Boltzmann equation as follows:

$$\nabla^2\psi(\mathbf{x}) = -\rho_{\text{fixed}}(\mathbf{x})/\varepsilon - qc_0 \exp(-q\psi(\mathbf{x})/k_BT)/\varepsilon \tag{2.27}$$

One of the drawbacks of the Poisson–Boltzmann model is that, at short distance, e.g. within a few tenths of a nanometre from the membrane surface, the approximation of continuous charge density breaks down because of the atomistic nature of the system (Guldbrand et al., 1984; Redondo and Laser, 2004).

2.2.1.3 Fixed Charge Group

The capability of achieving large volume transition for the hydrogel is facilitated by the weakly acidic or weakly basic groups bound onto the polymer network chains, which is strongly dependent on the dissociation constant. The groups are readily ionizable and sensitive to the environment pH surrounding the hydrogel

(Katchalsky, 1949; Fragala et al., 1972; Tanaka et al., 1980; De Rossi et al., 1985). For example, the weakly acidic carboxyl groups exist in form of R–COOH when the hydrogen ion H^+ concentration is higher than the dissociation constant K_a, whereas the pendent groups are charged and become R–COO^- if the H^+ concentration of medium is lower than K_a, which is characterized by

$$\text{R–COOH} \rightleftharpoons \text{R–COO}^- + \text{H}^+ \tag{2.28}$$

Therefore, the hydrogen ion H^+ is an important controller for electrochemical modulation of swelling of the pH-sensitive hydrogel. A relation between the fixed charge groups and the diffusive hydrogen ions was developed according to the Langmuir adsorption isotherm (Grimshaw et al., 1990). Based on the mechanism of single site binding single ion, the equilibrium constant is defined as follows:

$$K_a = \frac{[\text{R–COO}^-][\text{H}^+]}{[\text{R–COOH}]} \tag{2.29}$$

The density of total ionizable fixed charge groups within the dry gel is determined by titration process per volume of solid polymer (Grimshaw, 1989) and given as

$$c^s_{m0} = \frac{\text{moles of ionizable group}}{\text{volume of solid polymer}} = \frac{n}{V^s} \tag{2.30}$$

Since the ionic concentrations in Eqs. (2.1) and (2.2) are averaged over the interstitial fluid volume, we need to convert the density of total ionizable groups c^s_{m0} in a single unit of fluid volume:

$$c_{m0} = \frac{n}{V^f} = c^s_{m0}\frac{V^s}{V^f} = \frac{c^s_{m0}}{H} \tag{2.31}$$

where H is the hydration of the hydrogel and defined as the ratio of the interstitial fluid volume V^f to the solid polymer volume V^s as follows:

$$H = \frac{\text{volume of interstitial fluid}}{\text{volume of solid polymer}} = \frac{V^f}{V^s} \tag{2.32}$$

The reaction isotherm is described by

$$K_a = \frac{c_f c_{\text{H}^+}}{c_{m0} - c_f} \tag{2.33}$$

After rearrangement, the concentration of the fixed charge groups bound on the polymer chains, c, is finally written in the following form for an anionic hydrogel:

$$c_f = \frac{K_a c_{m0}}{K_a + c_{\text{H}^+}} = \frac{c^s_{m0}}{H}\frac{K_a}{K_a + c_{\text{H}^+}} \tag{2.34}$$

The above relation between the fixed charge density and the diffusive hydrogen ion concentration can be employed for computing the concentration of the fixed charge groups, as a function of the concentration of total ionizable groups in the dry gel, c^s_{m0}, and the concentration of free hydrogen ion c_{H^+} (Siegel et al., 1991; Siegel, 1990).

For a cationic hydrogel, the fixed charge density c_f based on the Langmuir isotherm relation is derived as

$$c_f = \frac{c^s_{m0}}{H} \frac{c_{\mathrm{H}^+}}{K_a + c_{\mathrm{H}^+}} \tag{2.35}$$

It should be noted that the fixed charge groups are bound onto the polymeric network chain and thus become immobile. In general, the profiles of the fixed charge groups are modified only by chemical reaction (Shibayama and Tanaka, 1993; Shiga et al., 1992a, b).

2.2.2 Mechanical Formulation

As mentioned before, the smart hydrogels are able to absorb or exude the fluid where they are immersed and thus swell or deswell until equilibrium is attained. At equilibrium state, the swelling force is balanced by the elastic retractive force exerted by crosslinked polymer solid matrix network of the hydrogel in order to maintain the current hydration state. The total swelling force could arise from the stretching of electrostatic effect, the polymer–solvent and polymer–solute interactions and entropic effect (Flory, 1962). However, it is known that the swelling force arising from the entropic effect, e.g. thermal motion or solvent interactions, reaches steady state faster than the ionic diffusion or water flow. Thus the swelling stress could be a state function of ionic environmental condition, and the hydration and fixed charge of the hydrogels. In this section, the mechanical equilibrium governing equations are formulated for swelling/deswelling deformation of the charged hydrogel.

As well known, usually the pH-sensitive hydrogel undergoes large deformation due to the effects of chemo-electro-mechanical multi-energy coupled fields, especially at higher pH level of surrounding solution. Then the difference between the initial and deformed configurations cannot be neglected as it is done for analysis of linear elasticity. The deformation gradient tensor $\boldsymbol{F}$ is thus defined as

$$\mathbf{F} = F_{ij} = \frac{\partial x_i^{\text{Deformed Configuration}}}{\partial X_j^{\text{Initial Configuration}}} = \frac{\partial (X_i + u_i)}{\partial X_j} = \delta_{ij} + \frac{\partial u_i}{\partial X_j} = \mathbf{I} + \nabla \cdot \mathbf{u} \tag{2.36}$$

For analysis of geometrically nonlinear problems, the mechanical governing equation of large deformation based on a total Lagrangian description is given as

$$\nabla \cdot \boldsymbol{P} + \boldsymbol{b} - \rho \dot{\boldsymbol{U}} = \boldsymbol{f} \tag{2.37}$$

where $\boldsymbol{P}$ is the first Piola–Kirchhoff stress tensor, ρ is membrane density, $\boldsymbol{b}$ is body force, $\boldsymbol{f}$ is external force, $\dot{\boldsymbol{U}}$is acceleration and $\rho\dot{\boldsymbol{U}}$ is inertial force. In the present mechanical analysis, no external force is considered so that $\boldsymbol{f}$=0, and the effects of $\boldsymbol{b}$ and $\rho\dot{\boldsymbol{U}}$ are neglected. Thus,

$$\nabla \cdot \boldsymbol{P} = 0 \text{ in } \Omega \tag{2.38}$$

$$\boldsymbol{u} = \boldsymbol{u}^* \text{ in } \Gamma_{\boldsymbol{u}^*} \tag{2.39}$$

$$\boldsymbol{P} \cdot \boldsymbol{n} = \boldsymbol{s}^* \text{ in } \Gamma_{\boldsymbol{s}^*} \tag{2.40}$$

where $\boldsymbol{u}^*$ is the specified displacement vector on the boundary portion $\Gamma_{\boldsymbol{u}*}$, $\boldsymbol{s}^*$ is the surface traction vector on the boundary $\Gamma_{\boldsymbol{s}*}$ and $\boldsymbol{n}$ is the unit outward normal vector. $\boldsymbol{u}$ is the displacement vector from the initial configuration $\boldsymbol{X}$ to the deformed configuration $\boldsymbol{x}$ where $\boldsymbol{x}$= $\boldsymbol{X}$+u. P as the first Piola–Kirchhoff stress tensor is a kind of expatriate, living partially in the deformed configuration $\boldsymbol{x}$ and partially in the reference configuration $\boldsymbol{X}$. Usually the second Piola–Kirchhoff stress $\boldsymbol{S}$ and the Green–Lagrangian strain $\boldsymbol{E}$ are used as the stress and strain measurements, respectively.

As $\boldsymbol{P}$ is unmeasurable and asymmetrical, the second Piola–Kirchhoff stress tensor $\boldsymbol{S}$ is required because $\boldsymbol{S}$ is symmetric and it is often used as the stress measurement (Malvern, 1969). For continuous solid materials, the relation between the first Piola–Kirchhoff stress tensor $\boldsymbol{P}$ and the second Piola–Kirchhoff stress tensor $\boldsymbol{S}$ is given as

$$\boldsymbol{P} = \boldsymbol{S}\boldsymbol{F}^{\mathrm{T}} \tag{2.41}$$

For the present hydrogel as a porous mixture, the above relation could be modified as follows:

$$\boldsymbol{P} = -J\boldsymbol{F}^{-1}p_{\text{osmotic}}\boldsymbol{I} + \boldsymbol{S}\boldsymbol{F}^{\boldsymbol{T}} \tag{2.42}$$

where $J = \det(\mathbf{F})$ is the determinant of deformation gradient tensor $\boldsymbol{F}$, p_{osmotic} is the osmotic pressure and $\boldsymbol{I}$ is identity tensor. One can also have

$$\boldsymbol{S} = \boldsymbol{C}{:}\boldsymbol{E} \text{ or } S_{ij} = C_{ijkl}E_{kl} \tag{2.43}$$

where C is the material moduli tensor and $\boldsymbol{E}$ is the Green–Lagrangian strain tensor used as strain measurement (here the symbol (:) in $\boldsymbol{A}{:}\boldsymbol{B}$ is the double contraction of inner indices, namely $\boldsymbol{A}{:}\boldsymbol{B}$ is given by $\boldsymbol{A}_{ij}\boldsymbol{B}_{ij}$. If $\boldsymbol{A}$ or $\boldsymbol{B}$ is symmetric, $\boldsymbol{A}{:}\boldsymbol{B}$= $\boldsymbol{A}_{ij}\boldsymbol{B}_{ji}$).

If the material is elastically isotropic

$$S_{ij} = [\lambda\delta_{ij}\delta_{kl} + \mu(\delta_{ik}\delta_{jl} + \delta_{il}\delta_{jk})]E_{kl} \tag{2.44}$$

Specially in one-dimensional domain

$$S_{11} = (\lambda + 2\mu)\left[\frac{1}{2}\left(2\frac{du}{dX} + \left(\frac{du}{dX}\right)^2\right)\right] = (\lambda + 2\mu)\left[\frac{du}{dX} + \frac{1}{2}\left(\frac{du}{dX}\right)^2\right] \tag{2.45}$$

For isotropic elastic materials, the material moduli tensor can be written as

$$C = \lambda I \otimes I + 2\mu I \quad \text{or} \quad C_{ijkl} = \lambda \delta_{ij}\delta_{kl} + \mu \left(\delta_{ik}\delta_{jl} + \delta_{il}\delta_{jk}\right) \tag{2.46}$$

where λ and μ are the Lamé coefficients of solid phase (here the symbol $\otimes$ in $a \otimes b$ indicates the vector product. In indicial notation, $a \otimes b \rightarrow a_i b_j$. In matrix notation, $a \otimes b \rightarrow \{a\}\{b\}^{\mathbf{T}}$). For example, in two-dimensional domain, there are two kinds of typical problems, the plane strain and plane stress problems.

In the plane strain problem, the thickness of solids in the z-direction is very large, compared with dimensions in the x- and y-directions. External loading is applied uniformly along the z-axis, and the movement in the z-direction at any point is constrained. The strain components in z-direction (ε_{zz}, ε_{xz}, ε_{yz}) are all zero, and there are only three in-plane strains (ε_{xx}, ε_{yy}, ε_{xy}) to deal with. Then

$$\mathbf{C} = \frac{E}{(1+\nu)(1-2\nu)} \begin{bmatrix} 1-\nu & \nu & 0 \\ \nu & 1-\nu & 0 \\ 0 & 0 & (1-2\nu)/2 \end{bmatrix} \text{ or } \mathbf{C} = \begin{bmatrix} \lambda + 2\mu & \lambda & 0 \\ \lambda & \lambda + 2\mu & 0 \\ 0 & 0 & \mu \end{bmatrix} \tag{2.47}$$

In the plane stress problem, however, the thickness of solids in the z-direction is very small, compared with dimensions in the x- and y-directions. As external forces are applied only within the x–y plane and the stress components in z-direction (σ_{zz}, σ_{xz}, σ_{yz}) are all zero, there are only three in-plane stresses (σ_{xx}, σ_{yy}, σ_{xy}) to deal with. Then

$$C = \frac{E}{(1-\nu^2)} \begin{bmatrix} 1 & \nu & 0 \\ \nu & 1 & 0 \\ 0 & 0 & (1-\nu)/2 \end{bmatrix} \tag{2.48}$$

where the two Lamé elastic constants, λ and μ, are associated with the shear modulus G, Young's modulus E and Poisson's ratio v as follows:

$$\lambda = \frac{\nu E}{(1+\nu)(1-2\nu)} \text{ and } \mu = G = \frac{E}{2(1+\nu)} \tag{2.49}$$

The Green–Lagrangian strain tensor $\boldsymbol{E}$ is given by

$$\boldsymbol{E} = \frac{1}{2}(\boldsymbol{F}^{\boldsymbol{T}} \cdot \boldsymbol{F} - \boldsymbol{I}) \text{ or } E_{ij} = \frac{1}{2}(F_{ik}^{T} F_{kj} - \delta_{ij}) = \frac{1}{2}\left(\frac{\partial u_i}{\partial X_j} + \frac{\partial u_j}{\partial X_i} + \frac{\partial u_k}{\partial X_i}\frac{\partial u_k}{\partial X_j}\right) \tag{2.50}$$

For example, in two-dimensional domain

$$\boldsymbol{E} = E_{ij} = \frac{1}{2} \begin{bmatrix} 2\frac{\partial u_1}{\partial X_1} + \left(\frac{\partial u_1}{\partial X_1}\right)^2 + \left(\frac{\partial u_2}{\partial X_1}\right)^2 & \frac{\partial u_1}{\partial X_2} + \frac{\partial u_2}{\partial X_1} + \frac{\partial u_1}{\partial X_1}\frac{\partial u_1}{\partial X_2} + \frac{\partial u_2}{\partial X_1}\frac{\partial u_2}{\partial X_2} \\ \frac{\partial u_1}{\partial X_2} + \frac{\partial u_2}{\partial X_1} + \frac{\partial u_1}{\partial X_1}\frac{\partial u_1}{\partial X_2} + \frac{\partial u_2}{\partial X_1}\frac{\partial u_2}{\partial X_2} & 2\frac{\partial u_2}{\partial X_2} + \left(\frac{\partial u_2}{\partial X_2}\right)^2 + \left(\frac{\partial u_1}{\partial X_2}\right)^2 \end{bmatrix} \tag{2.51}$$

Therefore, the momentum equilibrium equation for the hydrogel mixture can be finally written as

$$\nabla \cdot (-J\boldsymbol{F}^{-1} p_{\text{osmotic}} \boldsymbol{I} + \boldsymbol{S}\boldsymbol{F}^{\boldsymbol{T}}) = 0 \tag{2.52}$$

For example, in two-dimensional domain

$$\begin{aligned} \boldsymbol{P} &= -J\boldsymbol{F}^{-1} p_{\text{osmotic}} \boldsymbol{I} + \boldsymbol{S}\boldsymbol{F}^{T} \\ &= -p_{\text{osmotic}} \begin{bmatrix} 1 + \frac{\partial u_2}{\partial X_2} & -\frac{\partial u_1}{\partial X_2} \\ -\frac{\partial u_2}{\partial X_1} & 1 + \frac{\partial u_1}{\partial X_1} \end{bmatrix} + \begin{bmatrix} S_{11} & S_{12} \\ S_{21} & S_{22} \end{bmatrix} \begin{bmatrix} 1 + \frac{\partial u_1}{\partial X_1} & \frac{\partial u_2}{\partial X_1} \\ \frac{\partial u_1}{\partial X_2} & 1 + \frac{\partial u_2}{\partial X_2} \end{bmatrix} \\ &= -p_{\text{osmotic}} \begin{bmatrix} 1 + \frac{\partial u_2}{\partial X_2} & -\frac{\partial u_1}{\partial X_2} \\ -\frac{\partial u_2}{\partial X_1} & 1 + \frac{\partial u_1}{\partial X_1} \end{bmatrix} \\ &\quad + \begin{bmatrix} S_{11}\left(1 + \frac{\partial u_1}{\partial X_1}\right) + S_{12}\frac{\partial u_1}{\partial X_2} & S_{11}\frac{\partial u_2}{\partial X_1} + S_{12}\left(1 + \frac{\partial u_2}{\partial X_2}\right) \\ S_{21}\left(1 + \frac{\partial u_1}{\partial X_1}\right) + S_{22}\frac{\partial u_1}{\partial X_2} & S_{21}\frac{\partial u_2}{\partial X_1} + S_{22}\left(1 + \frac{\partial u_2}{\partial X_2}\right) \end{bmatrix} \\ &= \begin{bmatrix} S_{11}\left(1 + \frac{\partial u_1}{\partial X_1}\right) + S_{12}\frac{\partial u_1}{\partial X_2} - p_{\text{osmotic}}\left(1 + \frac{\partial u_2}{\partial X_2}\right) & S_{11}\frac{\partial u_2}{\partial X_1} + S_{12}\left(1 + \frac{\partial u_2}{\partial X_2}\right) + p_{\text{osmotic}}\frac{\partial u_1}{\partial X_2} \\ S_{21}\left(1 + \frac{\partial u_1}{\partial X_1}\right) + S_{22}\frac{\partial u_1}{\partial X_2} + p_{\text{osmotic}}\frac{\partial u_2}{\partial X_1} & S_{21}\frac{\partial u_2}{\partial X_1} + S_{22}\left(1 + \frac{\partial u_2}{\partial X_2}\right) - p_{\text{osmotic}}\left(1 + \frac{\partial u_1}{\partial X_1}\right) \end{bmatrix} \end{aligned} \tag{2.53}$$

$$\nabla \cdot \boldsymbol{P} = 0 \Rightarrow \begin{bmatrix} \dfrac{\partial}{\partial X_1}\left[S_{11}\left(1+\dfrac{\partial u_1}{\partial X_1}\right)+S_{12}\dfrac{\partial u_1}{\partial X_2}-p_{\text{osmotic}}\left(1+\dfrac{\partial u_2}{\partial X_2}\right)\right] \\ \quad +\dfrac{\partial}{\partial X_2}\left[S_{21}\left(1+\dfrac{\partial u_1}{\partial X_1}\right)+S_{22}\dfrac{\partial u_1}{\partial X_2}+p_{\text{osmotic}}\dfrac{\partial u_2}{\partial X_1}\right] \\ \dfrac{\partial}{\partial X_1}\left[S_{11}\dfrac{\partial u_2}{\partial X_1}+S_{12}\left(1+\dfrac{\partial u_2}{\partial X_2}\right)+p_{\text{osmotic}}\dfrac{\partial u_1}{\partial X_2}\right] \\ \quad +\dfrac{\partial}{\partial X_2}\left[S_{21}\dfrac{\partial u_2}{\partial X_1}+S_{22}\left(1+\dfrac{\partial u_2}{\partial X_2}\right)-p_{\text{osmotic}}\left(1+\dfrac{\partial u_1}{\partial X_1}\right)\right] \end{bmatrix} = 0 \tag{2.54}$$

Specially for one-dimensional analysis

$$\nabla \cdot \boldsymbol{P} = \nabla \cdot (-J\boldsymbol{F}^{-1}p_{\text{osmotic}}\boldsymbol{I} + \boldsymbol{S}\boldsymbol{F}^{T}) = \frac{d}{dX}\left[-p_{\text{osmotic}} + S_{11}\left(1+\frac{du}{dX}\right)\right] = 0 \tag{2.55}$$

that is

$$\begin{aligned} &\frac{d}{dX}\left[-p_{\text{osmotic}} + (\lambda+2\mu)\left[\frac{du}{dX}+\frac{1}{2}\left(\frac{du}{dX}\right)^2\right]\left(1+\frac{du}{dX}\right)\right] = 0 \\ &(\lambda+2\mu)\left[\frac{d^2u}{dX^2}+3\frac{du}{dX}\frac{d^2u}{dX^2}+\frac{3}{2}\left(\frac{du}{dX}\right)^2\frac{d^2u}{dX^2}\right] - \frac{dp_{\text{osmotic}}}{dX} = 0 \end{aligned} \tag{2.56}$$

The multiphase hydrogels may behave small deformation if the pH value of bathing solution is low. Then the linear elastic theory may provide sufficiently accurate simulation, and thus Eq. (2.52) is simplified to (Lai et al., 1991)

$$\nabla \cdot \sigma = \nabla \cdot [\lambda(\text{tr}(\boldsymbol{E}))\boldsymbol{I} + 2\mu\boldsymbol{E} - p_{\text{osmotic}}\boldsymbol{I}] = 0 \tag{2.57}$$

where $\boldsymbol{\sigma}$ is the Cauchy stress tensor. p_{osmotic} is the osmotic pressure contributed by the tendency of the hydrogel to absorb additional solvent, which is formulated by the difference of the concentrations between the interior hydrogel and the external medium (Helfferich, 1962; Katchalsky and Curran, 1965). Hence the osmotic pressure can be calculated according to

$$p_{\text{osmotic}} = RT\sum_k (c_k - \bar{c}_k) \tag{2.58}$$

where $\bar{c}_k$ is the concentration of the kth ion species in external solution and c_k the concentration of the kth ion species within the hydrogel.

2.3 Computational Domain, Boundary Condition and Numerical Implementation

In this section, the appropriate electrochemical and mechanical boundary conditions are specified to implement the MECpH model, which are associated with the experimental work conducted by Beebe and his team (Beebe et al., 2000a; De et al., 2002). In their experiment, the hydrogels were fabricated in a microchannel with upper and lower surfaces covered with glasses so that the deformation of hydrogels in axial direction was confined and the swelling occurs only in the radial direction. Due to the constraints, the equilibrium swelling/shrinking of a cylindrical hydrogel can be modelled as a one-dimensional problem along the diameter of the hydrogel. If the constant concentrations of surrounding bath solution and the macroscopic homogenous properties of the hydrogel are assumed, the one-dimensional problem can be further simplified to a symmetrical problem about the axis of the cylindrical hydrogel. Because of the axisymmetry, only half of the diameter is required in simulation, as shown in Fig. 2.1. In summary, the one-dimensional computational domain is thus composed of three subdomains, namely the radius of the hydrogel which represents the interior cylindrical hydrogel, the surrounding solution along the radius direction which represents the exterior bathing medium and the boundary effect domain that refers to the hydrogel–solution interface. For a system of N

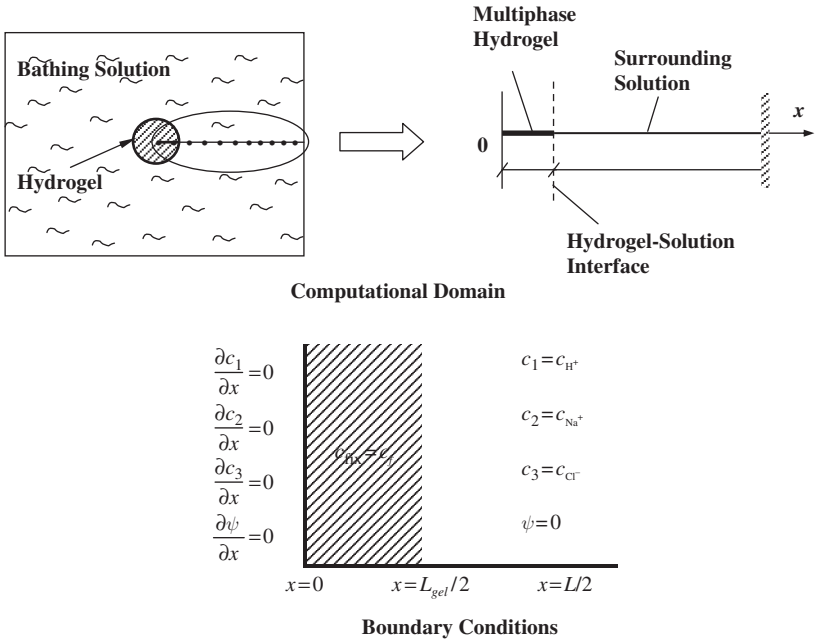

Fig. 2.1 Computational domain and boundary conditions for the numerical simulations, where the *shaded areas* represent the cylindrical pH-responsive hydrogel

diffusive species, the MECpH model generates the N Nernst–Planck equations (2.2) coupled with the Poisson equation (2.24). As usual, all the simulations are subjected to ambient temperature or stated otherwise.

Since this is an axisymmetric problem, the Neumann type of electrochemical boundary conditions is imposed within the hydrogel for continuity and the Dirichlet boundary conditions are applied at solution edges as prescribed by the experiment. Furthermore, the boundary conditions for mechanical equilibrium are imposed at the hydrogel–solution interface. These boundary conditions are illustrated in Fig. 2.1.

It should be pointed out that the MECpH model can also be employed for simulation of the pH and electric coupled driven hydrogel, for example, when a hydrogel strip is immersed in pH buffered solution and centred between a pair of electrodes and aligned in parallel with them, where a DC electric field is applied across the domain. Then we can stimulate the degree of swelling/deswelling of the charged hydrogels subject to the coupled stimuli of chemical pH milieu and DC electric field. Due to the electric voltage applied across the system, the symmetric conditions are no longer applicable. The computational domain has to cover whole domain of interest, from the cathode on the left region to the anode on the right, where the boundary conditions of ionic concentrations are identical for each species in both the anode and cathode regions, i.e. $c_k^*=c_k^{\text{Left}}=c_k^{\text{Right}}$. The electric boundary conditions are given as prescribed by the applied electric voltage.

The MECpH model consisting of a set of nonlinear coupled electrochemical and mechanical equations has been developed for simulation of the swelling/deswelling equilibrium of the pH-sensitive hydrogel. Modelling of equilibrium behaviour of the pH-responsive hydrogel requires a good understanding of the diffusion of hydrogen ions inside and outside the hydrogel. This requirement also takes into account the chemical reactions of the hydrogen ions with the fixed charge groups and the buffering effect on the diffusion of hydrogen ion. Equations (2.2) coupled with Eq. (2.24) form a famous formulation known as Poisson–Nernst–Planck (PNP) system, expressed by a set of nonlinear partial differential equations. The PNP theory of continuum diffusion attempts to characterize the average ion fluxes in terms of the gradients of concentrations and/or electric potential. Based on the difference in the ionic concentrations and electric potential across the hydrogel, the degree of equilibrium swelling/shrinking can be computed by the finite deformation mechanical governing equation (2.52) or (2.57).

It is definitely impossible for the MECpH model to have any closed-form analytical solutions, which is composed of the PNP system (2.2) and (2.24) coupled with the mechanical equation (2.52) or (2.57). We have to employ appropriate numerical approaches for approximate solutions of the MECpH model. A strong-form meshless numerical technique termed the Hermite-cloud method is thus used (Li et al., 2003), which faces several computing challenges of the MECpH model, such as the remeshing of computational domain due to moving boundaries at the hydrogel–solution interfaces and the localized high gradient over the hydrogel–solution

interfaces. For simplification of numerical computation, a set of non-dimensional parameters is defined as follows:

$$\tilde{x} = \frac{x}{L_{\text{ref}}}, \tilde{u} = \frac{u}{L_{\text{ref}}}, \tilde{c}_k = \frac{c_k}{c_{\text{ref}}}, \tilde{c}_f = \frac{c_f}{c_{\text{ref}}}, \tilde{\psi} = \frac{\psi}{\psi_{\text{ref}}} = \frac{F\psi}{\eta RT} \tag{2.59}$$

where $\tilde{x}$, $\tilde{u}$, $\tilde{c}_k$, $\tilde{c}_f$, $\tilde{\psi}$ are the dimensionless variables of coordinate, displacement, diffusive ionic concentration, fixed charge density and electric potential, respectively. L_{ref}, c_{ref}, ψ_{ref} and η are the characteristic length, concentration, electric potential and weighted coefficient, respectively. As a result, the non-dimensional form of the MECpH governing equations can be written to simplify numerical simulation. Another reason for the non-dimensional treatment is to overcome the difficulty of the unknown variables with different scales and units.

Computational flowchart is illustrated in Fig. 2.2. By following the flowchart, the fixed charge density c_f is computed first by Eq. (2.34) or (2.35), followed by solving the Nernst–Planck equations (2.2) and Poisson equation (2.24) with a Newton iterative technique and a relaxation approach to the self-consistent PNP system for convergences of the mobile ionic concentrations c_k and the electric potential ψ. Both the converged concentrations c_k and potential ψ are in turn substituted into the mechanical equilibrium equation (2.52) or (2.57) for determining the corresponding displacement u of the hydrogel. Because of the deformation u, the fixed charge density c_f is redistributed within the hydrogel and thus this requests new computation again. This computational loop is carried out until all the independent variables converge, including the diffusive ionic concentrations $c_k(k = 1,2,3,...,N_{\text{ion}})$ and the electric potential ψ as well as the hydrogel displacement u.

The swelling/deswelling of the pH-sensitive hydrogel in equilibrium can be predicted by the steady-state simulation based on the Nernst–Planck equations, the Poisson equation and the mechanical equilibrium governing equation, collectively known as MECpH model. The set of equations is amenable by numerical solution. Nevertheless, appropriate approximations can greatly reduce the computing time necessarily for the solution with desired accuracy.

First, the diffusion coefficients are eliminated in the steady-state simulation as they affect the diffusing rate only but not the final equilibrium state. In other words, the time derivative term, $\partial c_k/\partial t$, in Eq. (2.2) is removed for the steady-state simulation. This significantly reduces the computational cost when solving the system of coupled nonlinear partial differential equations, as the computing time is saved for transient solutions of the N continuity equations (2.2). Moreover, it is observed in many experiments that the diffusion coefficient varies slightly with change in the degree of swelling (Gehrke and Cussler, 1989). Second, the convection term in the Nernst–Planck flux equations (2.2) is negligible as the fluid pressure remains constant across the hydrogel and the fluid velocity is unchanged with swelling of the hydrogel. This in fact assumes that the change in the concentration profiles due to convective flow of ions is much smaller than the concentrations resulting from the fluxes of diffusion and migration (Grimshaw, 1989). Third, it is also assumed

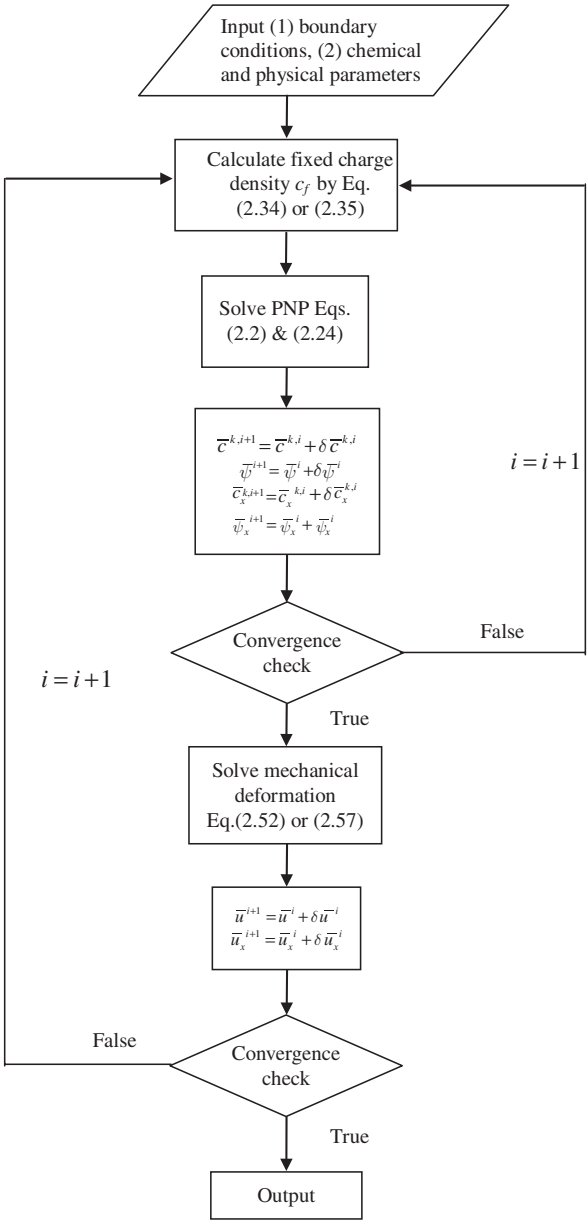

Fig. 2.2 Computational flowchart of relaxation approach for the self-consistent MECpH model

that the flux due to the chemical reaction of ions is much smaller than the net diffusion and migration fluxes. Therefore, the contribution of the chemical activity coefficient to the flux becomes negligible. In addition, the chemical activity coefficients of ionic species are always equal to unity in the dilute condition (Bockris

and Reddy-Amulya, 1998). Lastly, the properties of the hydrogel considered are assumed to be homogeneous so that only the isotropic equilibrium swelling occurs. Although the actual dielectric constants of ions depend on the species and applied electric current, they are chosen equally each other for simplification. Besides that, electrolytic process due to the externally applied electric field can be ignored by limiting to low-range voltages in simulations.

In summary, for implementation of the MECpH model, the mechanical equilibrium governing equation (2.52) or (2.57) is coupled with the PNP equations (2.2) and (2.24) and the fixed charge dissociation equation (2.34) or (2.35) through the local hydration H. These equations complete the MECpH model. Therefore, there are N_{ion} Nernst–Planck equations (2.2) coupled with the Poisson equation (2.24) for the (N_{ion}+1) unknown variables $c_1, c_2, \ldots, c_N, \psi$. Apart from that, the mechanical equilibrium governing equation (2.52) or (2.57) is solved for the (N_{ion}+2)th unknown variable, i.e. the deformation u of the hydrogel. If appropriate boundary conditions are specified, these equations construct a complete partial differential boundary value (PDBV) problem with (N_{ion}+2) unknown variables. In principle, these equations can be solved approximately for the concentrations of diffusive species and fixed charge group, the electric potential and displacement. However, these equations are coupled nonlinearly which complicates the computation of the MECpH model.

2.4 Model Validation with Experiment

In order to examine the MECpH model, one-dimensional steady-state simulations are conducted and compared with the experimental data obtained by Beebe and his group (Beebe et al., 2000, 2002; De et al., 2002). For illustration of the single dimensionality of the present problem, an insight is given into the experimental procedure. With reference to the experimental work by Beebe et al. (2000a), the polymerizable mixture, composed of acrylic acid and 2-hydroxyethyl methacrylate (HEMA) with the photoinitiator (3 wt%) and ethylene glycol dimethacrylate (1 wt%) as the crosslinker, was filled up in the microchannel where the experiment was carried out. The microchannel was covered at top and bottom with two pieces of glasses. When the mixture reached a quiescent state, it was exposed to UV light through a circular photomask placed on the top of the microchannel. The channel was then flushed with water to remove the unpolymerized monomers mixture. The axisymmetric cylindrical hydrogel was formed in the microchannel and constrained from axial displacement by the cover glasses placed on the top and bottom. Thus it is quite reasonable to assume that the cylindrical hydrogel undergoes displacement mainly in the radial direction. The cylindrical hydrogel with diameter of 400 μm at dry state was placed in a bathing solution with ionic strength of 300 mM. It was observed that the hydrogel swelled to a certain degree after submerged in the solution. The instantaneous swelling of the hydrogel is herein referred to as initial hydration state. The hydrogel was presumed to attain an equilibrium swelling state before it was

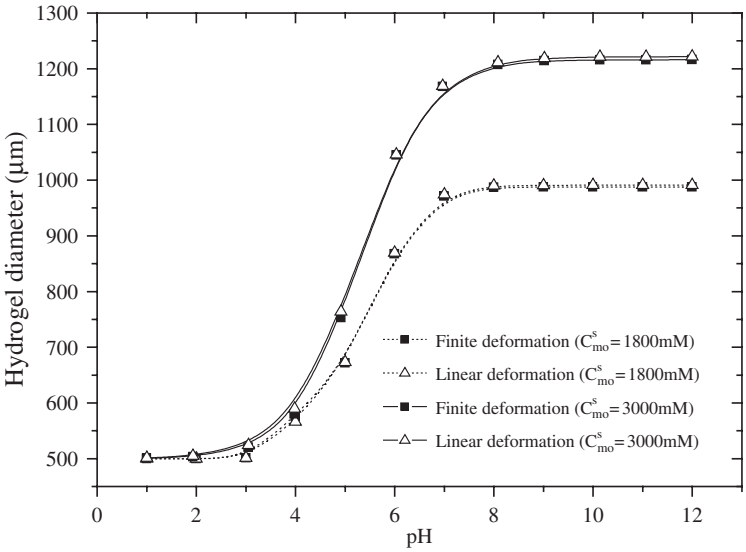

Fig. 2.3 Comparison of finite and linear deformation theories

subjected to step changes in pH of the surrounding solution. The volume changes of the hydrogel were observed and the diameter of the cylindrical hydrogel was measured after reaching equilibrium at various environmental pH values (circular markers in Fig. 2.4). Using the Hermite-cloud meshless technique (Li et al., 2003), the MECpH model, with the effects of chemo-electro-mechanical multi-energy fields expressed by fully coupled nonlinear partial differential equations, is solved numerically for simulation of the response performance of the given pH stimulus-responsive hydrogel. The simulation domain and corresponding boundary conditions are prescribed in Fig. 2.1.

Computations are conducted by both the finite and linear deformation theories for comparison. As shown in Fig. 2.3, the comparison between the two theories shows almost identical results. As the swelling of the hydrogel becomes larger, for example, when the ionizable fixed charge concentration increases, the linear deformation theory gives a slightly greater degree of swelling than that by the finite deformation theory.

The square markers in Fig. 2.4 indicate the simulation results obtained, where the solid line is plotted to assist visualization. It is apparent that they compare very well with the experimental data qualitatively and quantitatively. As well known, the change of environmental pH alters the degree of ionization of the fixed charge groups and the state of equilibrium swelling concurrently. The figure demonstrates that the hydrogel volume changes abruptly in the range from pH 4 to 7. It is also observed that the hydrogel remains almost unchanged from the initial hydrated state in the lower pH solution and starts to expand at about pH 4. As the pH of bathing solution increases, the ionization of the pendent poly(HEMA) carboxylic

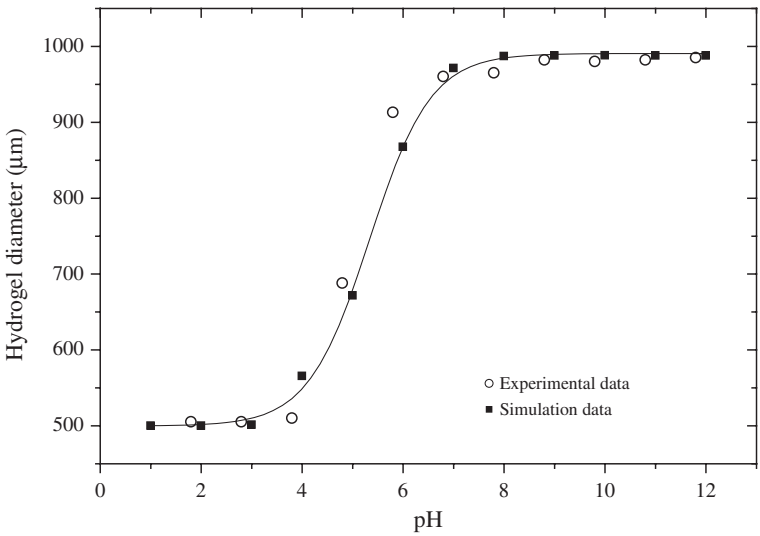

Fig. 2.4 Comparison between the experimental data (Beebe et al., 2000, 2002) and computational results by MECpH model for equilibrium swelling of the PHEMA hydrogel as function of pH

acid groups onto the backbone of the network increases, where the acid–base equilibrium process is described by the formula (2.28).

As a result, the surplus charge within the hydrogel increases. In order to maintain the neutrality within the hydrogel, more mobile ions with opposite sign to the fixed charge groups diffuse into the hydrogel. The concomitant increase of the ionic concentrations in the interior hydrogel generates higher osmotic pressure, which in turn causes the observable increase of swelling. As the ionization process of the carboxylic acid group approaches the saturation state at pH 7, the further increase of environmental pH after pH 7 does not enlarges significantly the degree of swelling. In summary, based on the above comparison and discussion of Fig. 2.4, it is concluded that the present MECpH model is accurate and robust to provide the prediction of the responsive behaviour of the pH-sensitive hydrogel with large deformation.

2.5 Parameter Studies by Steady-State Simulation for Equilibrium of Hydrogel

As mentioned before, the pH-sensitive hydrogel is the polymer network containing pendent ionizable groups which are usually weakly acidic or weakly basic. Ionization occurs when the environment pH changes, and then the pendent groups become charged. The responsive performance of the crosslinked charged hydrogel is mainly pH dependent. However, many effects also have to be considered, such as the crosslinking density, the chemical nature of the fixed charge groups, the ionic

strength and composition of bathing solution. They greatly affect the equilibrium swelling of the hydrogel (Brondsted and Kopecek, 1992).

Due to the intrinsic swelling property, the pH-sensitive hydrogel is explored for development of novel chemomechanical sensing system, which would convert chemical energy directly to mechanical work, for example, chemically driven functional actuator or sensor (Osada and Gong, 1993; Beebe et al., 2000a, b). The pH-sensitive hydrogel has significant advantages over conventional microfluidic actuators owing to the capability of undergoing the abrupt volume changes in response to surrounding environmental pH without requirement of external power source. In addition, the hydrogel can perform well for sensing, actuating and regulating functions that are usually performed by discrete components such as valve and sensor in traditional system.

Currently the applications of the smart hydrogels in medical and pharmaceutical fields are increasingly becoming one of the most active research areas. The pH-sensitive hydrogels are found to be appropriate carriers as swelling-controlled drug release devices. The ability to dynamically control the swelling of the hydrogels subject to the changes in the pH and ionic strength of the external medium provides various opportunities for the pH-sensitive hydrogels. For example, the pH of fluid varies considerably along the length of the gastrointestinal tract (1–3 in the stomach, 5–8 in the small intestine), a weakly acidic hydrogel is a good candidate as smart device to deliver drug into the small intestines while avoiding release in the stomach. Various drug delivery systems based on the pH-sensitive hydrogels are developed or reviewed by many researchers (Siegel, 1990; Lowman and Peppas, 1999; Peppas et al., 2000). Design and optimization of these systems greatly demand insight into the underlying mechanism of the equilibrium swelling of the smart hydrogels.

In this section, we pay our attention to parameter studies by steady-state simulation for equilibrium of the pH-responsive hydrogels. The emphasis is placed on the influences of various hydrogel material properties and surrounding environmental conditions on the equilibrium swelling responses of the pH-responsive hydrogels. They include the environmental pH, the physical properties of the hydrogel, the chemical nature of the fixed charge groups and the ionic strength and compositions of surrounding solution.

Simulations are worked out to discuss the influences of the hydrogel properties and bath conditions on the distributive profiles of diffusive ionic concentrations and electrical potential as well as mechanical displacement. The input data used for implementation of numerical simulations are tabulated in Table 2.1, which are obtained from the experimental works by Beebe's research group (Beebe et al., 2000a, b; Johnson et al., 2002, 2004a, b; Yu et al., 2001; Zhao and Moore, 2001) and the handbook (Lide, 2002).

As shown in Fig. 2.1, a cylindrical pH-sensitive hydrogel with circular cross-sectional area is immersed in a bath solution consisting of sodium chloride (NaCl) and hydrochloric acid (HCl), which is referred as ideal solution here. In order to investigate the influences of various buffer contents on the swelling equilibrium of the pH-sensitive hydrogel, two buffer solution systems, namely the phosphate buffer and the Britton–Robinson buffer, are considered. Advantage of using pH buffers in

Table 2.1 Essential chemical and physical parameters used as input data for implementation of the numerical simulations

K	$10^{-2.0}$mM
ν	0.45
ϵ	80
ϵ_0	8.8542×10^{-12}C^2/N·m^2
F	9.6487×10^4C/mol
T	298 K
R	8.314 J/mol·K

experiment is to stabilize the pH solution and swelling response rate, where the buffer may resist the change in the solution pH when small amount of acid or base is added. In general, a buffer solution is a mixture of weak acid or weak base and corresponding salt. For investigation of the influences of buffer content and hydrogel properties on the swelling equilibrium, the cylindrical hydrogels are placed into the two systems of the buffered solutions, namely the phosphate buffer and the Britton–Robinson buffer (Townshend, 1995). The phosphate buffer is prepared with the ionic strength specified by controlling NaCl, and the pH of the solution can be regulated by adding certain amount of NaH_2PO_4, Na_2HPO_4, HCl or NaOH. The Britton–Robinson buffer solution is prepared by mixing the specified amount of strong base NaOH with the solution containing weak acid CH_3COOH, H_3PO_4 and H_3BO_3 in a proportional amount until a desired pH value is attained. Usually the ionic strength and valence numbers of the diffusive ionic species have important effects that discern the difference between the phosphate and Briton–Robinson buffers. These effects are reflected clearly in the PNP equations (2.2) and (2.24) of the present MECpH model.

As mentioned before, the present problem domain is considered as axisymmetry so that the problem can be simplified to one-dimensional computation, where the swelling takes place along the radial direction of the cylindrical hydrogel, as shown in Fig. 2.1. Before swelling, the dry gel has diameter of 400 μm. In general, the diameter of the dry gel is determined by the diameter of the circular photomask. However, it is an inevitable consequence that the hydrogel dimensions vary from the size of the photomask after the microchannel is flushed to remove the unpolymerized monomers. Light scattering and reflection are identified by Beebe et al. (2000b) as the possible reasons behind the shift in the hydrogel dimension. Therefore, a boundary-effect domain is necessarily defined as describing the hydrogel–solution interface. Usually very short range is given as the length scale of the interface, for example, about 1/20 of the total length of the computational domain. As an example, at the state before swelling, $x(\mu m) \in [0, 200]$ is the interior dry gel domain and $x(\mu m) \in [300, 2000]$ is the solution domain. The hydrogel–solution interface, $x(\mu m) \in [200, 300]$, is referred to as the boundary-effect domain. A hyperbolic tangent profile is employed to polish the distribution of the fixed charge density, ranging from c_f within the hydrogel to zero in the bathing solution. The fixed charge concentration inside the hydrogel is calculated by Eq. (2.34) or (2.35) with $c^s_{m0} = 1800$ mM and $K = 10^{-2.0}$ mM, respectively. According to the experimental data obtained by

Beebe's research group (Johnson et al., 2002), it is well known that Young's modulus of the hydrogel varies with the environmental pH value. In similar manner to the fixed charge concentration, a hyperbolic tangent profile is used to polish the variation of Young's modulus as function of solution pH. The distributive profile of Young's modulus consists of three segments, namely constant Young's moduli of 0.29 MPa if pH$\leq$5.5 and 0.21 MPa if pH$\geq$7.5. In the third segment for 5.5<pH<7.5, Young's modulus is polished to vary linearly from 0.29 to 0.21 MPa.

Despite the complexity of the swelling/deswelling mechanism of the smart hydrogel at various levels of environmental pH, much insight can be obtained via independent investigations of the influences of various material properties of the hydrogel and the environmental conditions of the bath solution. The nonlinear coupled partial differential equations of the MECpH model are solved numerically with appropriate parameters to further understand the fundamental mechanism of the swelling or deswelling of the pH-sensitive hydrogels.

2.5.1 Influence of Initially Fixed Charge Density of Hydrogel

Figures 2.5, 2.6 and 2.7 are plotted for analysis of the distributive profiles of ionic concentrations, electric potential and mechanical displacement as functions of ionizable fixed charge density within the hydrogel.

Figure 2.5a–c shows the distributive patterns of the diffusive ionic concentrations of the hydrogen (H^+), sodium (Na^+) and chlorine (Cl^-) ions, when the hydrogel is submerged in the acidic solution of pH 3.0. The results simulated are intuitively correct in the sense that the PHEMA gel is an acidic hydrogel. The distributions of H^+ and Na^+ions are high in the hydrogel domain, but decreases in the bath solution; while the opposite characteristics are true for the Cl^- ion. The concentration of the H^+ ion is much lower than those of Na^+ and Cl^- ions. The electroneutrality is conserved at every point in the bath solution, which is proved straightforward from the summation of the concentration profiles in Fig. 2.5. In the interior hydrogel, there is a difference between the concentrations of the Na^+ and Cl^- ions, and the Na^+ ion has higher concentration. This concentration difference between the sodium and chlorine ions corresponds closely to the fixed charge concentration as shown in Fig. 2.5d. Figure 2.5e illustrates the distribution of electric potential. The net difference of drift forces among all ionic concentrations in the interior hydrogel results in a constant electric potential within the hydrogel, but it is usually very small, e.g. in millivolts. In the bath solution, however, the distributive electric potential is zero due to the electroneutrality resulting from the net resultant concentration of the all-ionic species. Figure 2.5f demonstrates the mechanical displacement of the cylindrical hydrogel in radial direction. It is seen that the degree of swelling of the hydrogel decreases by following the sequence of $c^s_{m0} = 2400$, 1800 and 1200 mM. It is predicted by the MECpH model that the PHEMA hydrogels with greater amount of initially fixed charge groups may exhibit greater swelling, even though the swelling

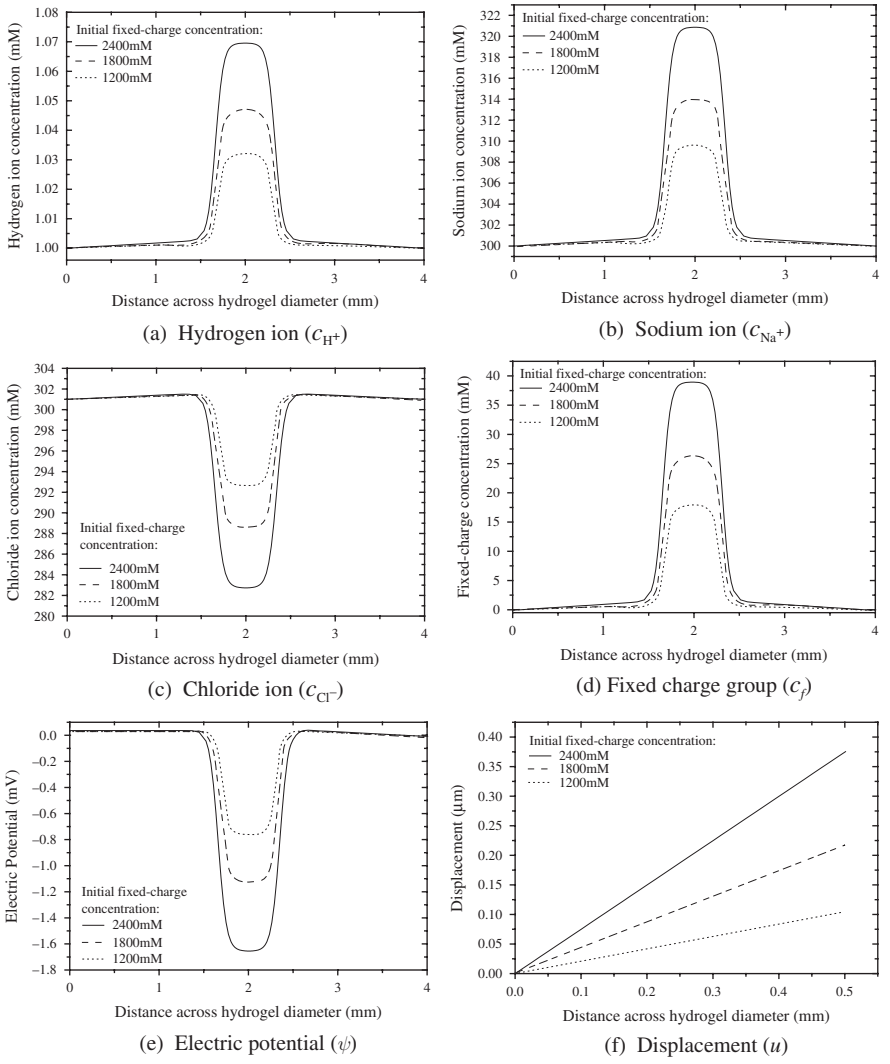

Fig. 2.5 Distributive profiles of $c_{H^+}, c_{Na^+}, c_{Cl^-}, c_f, \psi$ and u as the function of ionizable fixed charge concentration c^s_{mo}, where the PHEMA hydrogel is equilibrated in acidic medium of pH 3 with NaCl added to control the ionic strength

is very small in acidic solution as illustrated in Fig. 2.5, compared with that in basic solution as illustrated in Fig. 2.7.

Figures 2.6 and 2.7 demonstrate the distributive profiles of the diffusive ionic concentrations, electric potential and mechanical displacement of the hydrogel with the initial diameter of 400 μm in the neutral solution and the alkaline solution of pH 12 respectively, for the fixed charge groups at various initial concentrations. It is observed that the hydrogel behaves similar characteristics to those in

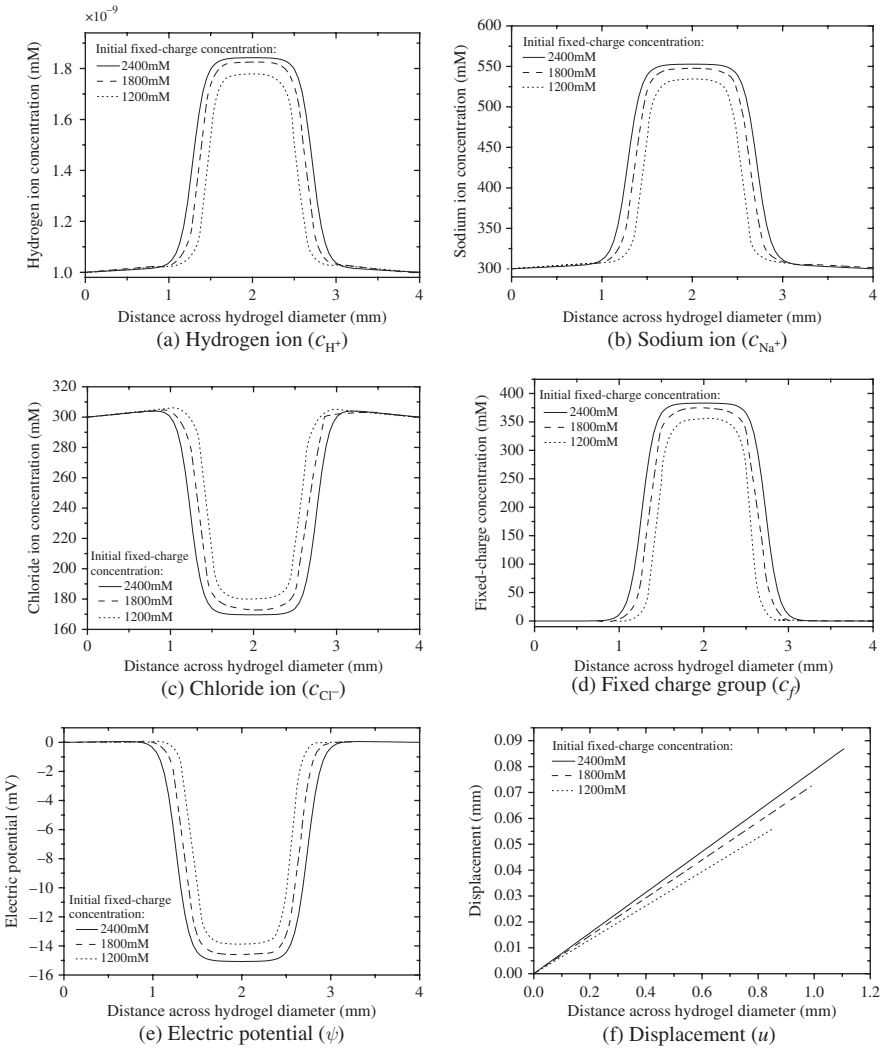

Fig. 2.6 Distributive profiles of c_{H^+},c_{Na^+},c_{Cl^-},c_f,ψ and u as the function of ionizable fixed charge concentration c^s_{mo}, where the PHEMA hydrogel is equilibrated in a neutral medium with NaCl added to control the ionic strength

the corresponding acidic bathing solution as shown in Fig. 2.5. However, there are dissimilarities quantitatively in the degree of swelling between the hydrogels when immersed in acidic and alkaline solutions. The degree of swelling of the PHEMA hydrogels is insignificant in acidic solution. In alkaline solution, however, they expand much more than the double size at dry state. On top of that, the differences in the degrees of swelling are also large among the hydrogels with different initially fixed charge densities.

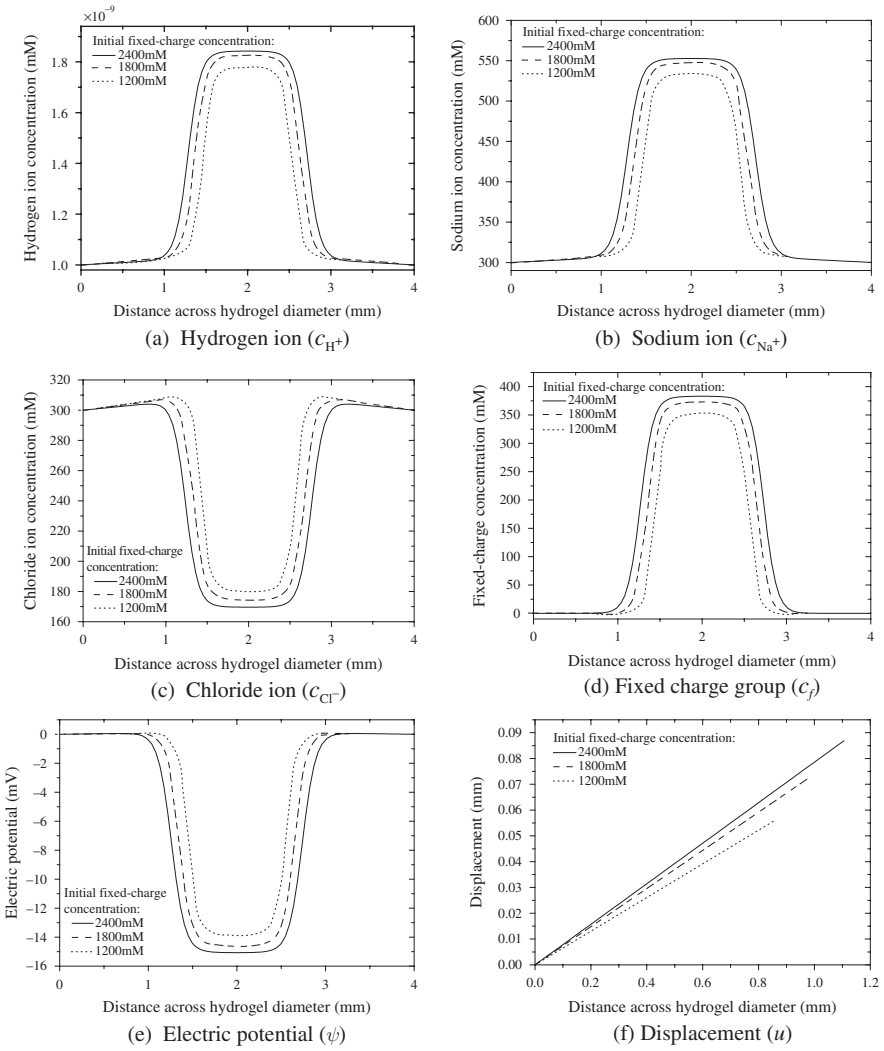

Fig. 2.7 Distributive profiles of c_{H^+},c_{Na^+},c_{Cl^-},c_f,ψ and u as the function of ionizable fixed charge concentration c^s_{mo}, where the PHEMA hydrogel is equilibrated in basic medium of pH 12 with NaCl added to control the ionic strength

The fixed charge groups attached onto the backbone of the PHEMA network, the carboxyl groups, exist in the form of R–COO^- in basic solution or in the form of R–COOH in acidic medium, which are characterized by Eq. (2.28). The dissociation constant K describes the ionization of the pendent fixed charge groups, like the acidic or basic groups of monobasics or monobases. If the concentration of the hydrogen ion H^+ is smaller than the dissociation constant K, the carboxyl groups try to release more protons. In order to maintain the electroneutrality, more mobile

counterions, e.g. Na^+in the present case, diffuse into the interior hydrogel to compensate the surplus charge. In contrast, the mobile anions are repulsed from entering the interior hydrogel. It is thus evident that the concentration of the Na^+ ion is higher whereas that of Cl^- ion is lower in the case of the alkaline solution, compared with the acidic solution. As a consequence, the concentration differences between the interior hydrogel and the exterior solution increase tremendously, leading to higher osmotic pressure which effectively drives higher degree of swelling.

Figure 2.8a, b shows the theoretically predicted dependence of the swelling of the pH-sensitive hydrogel response to the changes in the initially fixed charge density for an ideal solution at different pH levels. It is obvious that the change of the fixed charge concentration c^s_{m0} at dry state strongly influences the equilibrium swelling of the hydrogels at high pH values, whereby the decrease of c^s_{m0} dramatically reduces the degree of swelling at high pH values. The initial concentration of fixed charge c^s_{m0} is a function of molar ratio of the comonomers during preparation (Chu et al., 1995). As the molar ratio of carboxylic acid to 2-hydroxyethyl methacrylate decreases, the initially fixed charge density decreases dramatically. The concentration difference thus decreases between the interior hydrogel and the exterior solution. As a result, this in turn mitigates the osmotic pressure and generates smaller degree of hydrogel swelling. These observations are in agreement with the experimental trend reported by Siegel (1990). Figure 2.8b characterizes well the experimental phenomena, where a monotonic swelling is predicted with increasing the total molar concentration of ionizable groups per volume of solid network polymer.

Figure 2.9 exhibits the relation between the equilibrium swelling of the hydrogel and the concentration of fixed charge group c^s_{m0} for three different buffer solutions, the ideal solution, the phosphate buffer and the Briton–Robinson buffer. The larger c^s_{m0} is, the greater degree of swelling the hydrogel performs for both the buffer solutions at higher pH. At low pH level, however, the degree of swelling keeps almost constant for both the buffer systems. The figure evidently shows that the swelling equilibrium achievable in the Britton–Robinson system is always higher than that in the ideal solution and the phosphate buffer, especially as the initial concentration of fixed charge group c^s_{m0} increases highly. Swelling of the hydrogel is almost the same if bathed with either the phosphate buffer or the ideal solution, e.g. only NaCl and/or HCl in solution. However, the phosphate buffer shows greater degree of swelling with the increase of initially fixed charge group concentration c^s_{m0}.

2.5.2 Influence of Young's Modulus of Hydrogel

Figures 2.10, 2.11 and 2.12 are plotted for the distributions of ionic concentrations and electric potential as well as mechanical displacement as function of the normalized Young's modulus of the hydrogel, if placed in an ideal bathing solution composed of NaCl and HCl electrolytes. The characteristic profiles of the ionic concentrations and electric potential are similar to those in Figs. 2.5, 2.6 and 2.7 for environmental conditions of the acidic solution (pH 3), neutral solution (pH 7)

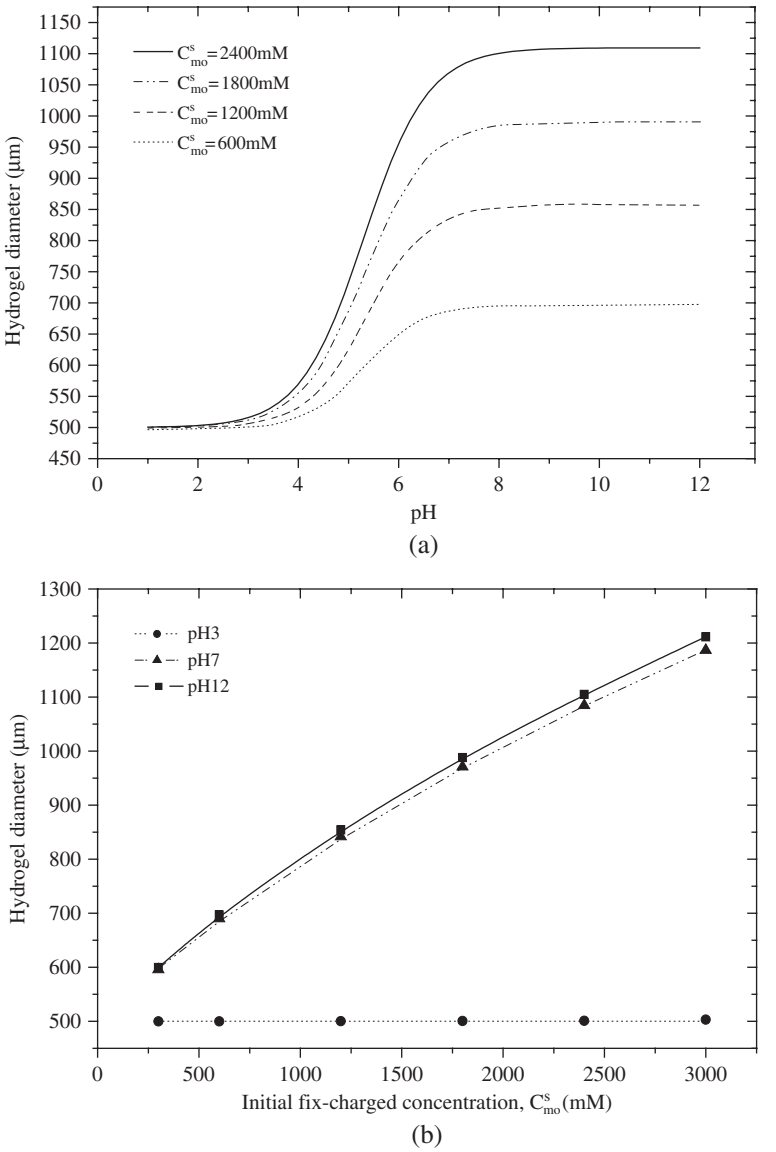

Fig. 2.8 Dependence of swelling on (**a**) bathing pH as the function of ionizable fixed charge concentration c^s_{mo} and (**b**) varying ionizable fixed charge concentrations c^s_{mo} in acidic, neutral and basic solutions

and basic solution (pH 12). The cationic concentrations, e.g. H^+ and Na^+ within the hydrogel are higher than those in the bath solution. In contrast, the anion concentration in the interior hydrogel is at a lower level than that in the external solution. Electroneutrality is conserved everywhere.

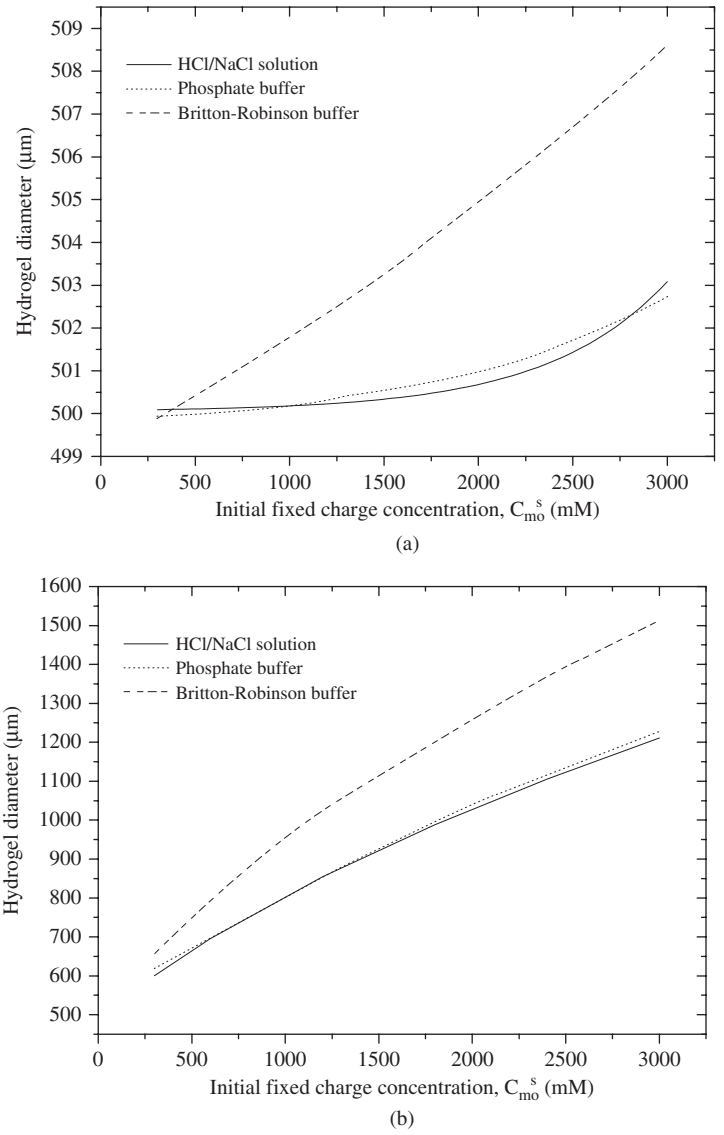

Fig. 2.9 Influences of buffer systems on swelling equilibrium as the function of ionizable fixed charge concentration in (**a**) acidic medium of pH 3 and (**b**) basic medium of pH 9

The dissimilarity of the swelling response at lower and higher pH levels displays two different conditions. As discerned from Fig. 2.10, the changes in Young's modulus values of the hydrogel seem to have no significant effect on the degree of swelling at low pH. Probably as the hydrogel is still in compact state at low pH, the effect of changing Young's modulus is very tiny on the swelling equilibrium. In contrast, the degree of swelling is controlled greatly by changing Young's modulus

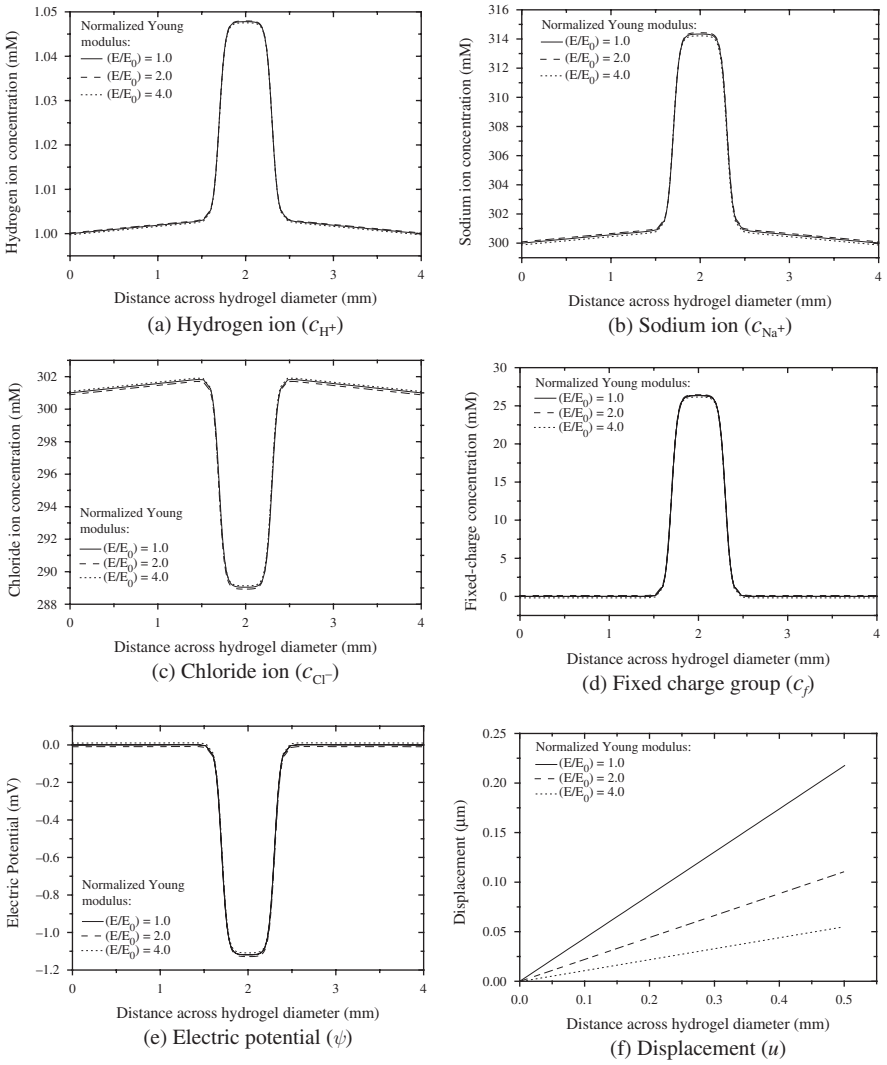

Fig. 2.10 Distributive profiles of c_{H^+},c_{Na^+},c_{Cl^-},c_f,ψ and u as the function of normalized Young's modulus (E/E_0), where the PHEMA hydrogel is equilibrated in acidic medium of pH 3 with NaCl added to control the ionic strength

if the environmental pH level is high, as observed from Figs. 2.11 and 2.12. The phenomena mentioned occur owing to the fact that the more fixed charge groups are ionized as pH increases and thus the degree of swelling increases. However, the swelling is constrained as Young's modulus increases. The interaction between expanding and retracting forces lasts until new equilibrium is reached.

Figure 2.13a shows the dependence of swelling of the hydrogel on the changes of environmental pH as function of Young's modulus of the pH-sensitive hydrogel.

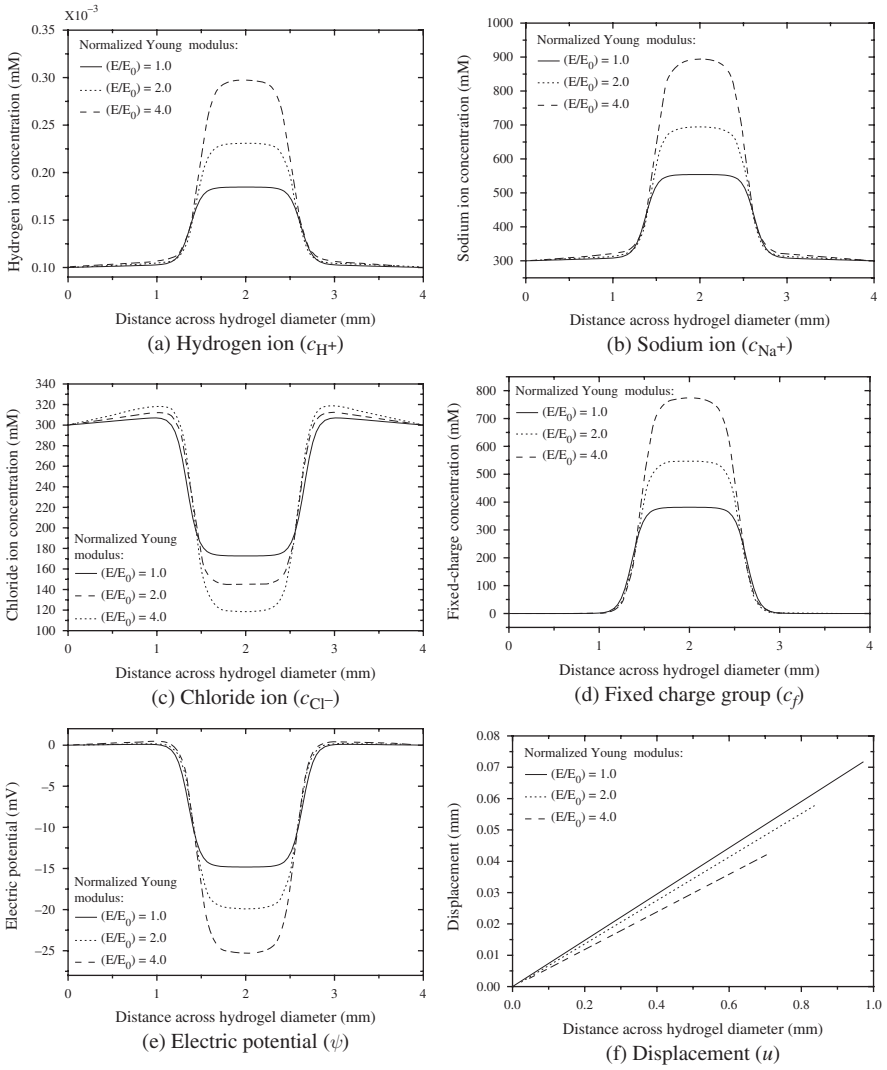

Fig. 2.11 Distributive profiles of c_{H}^{+},c_{Na}^{+},c_{Cl}^{-},c_f,ψ and u as the function of normalized Young's modulus (E/E_0) , where the PHEMA hydrogel is equilibrated in neutral medium with NaCl added to control the ionic strength

The MECpH model theoretically predicts that, for the hydrogels with larger Young's modulus, the degree of swelling decreases at higher solution pH. The characteristics become more visible in Fig. 2.13b when the normalized Young's modulus is plotted against the diameters of hydrogels at equilibrium state. The magnitude of swelling reduces exponentially with the increase of Young's modulus. Usually it is known that Young's modulus of the hydrogel is strongly dependent on preparation process, where the modulus is primarily determined by the volume per molar

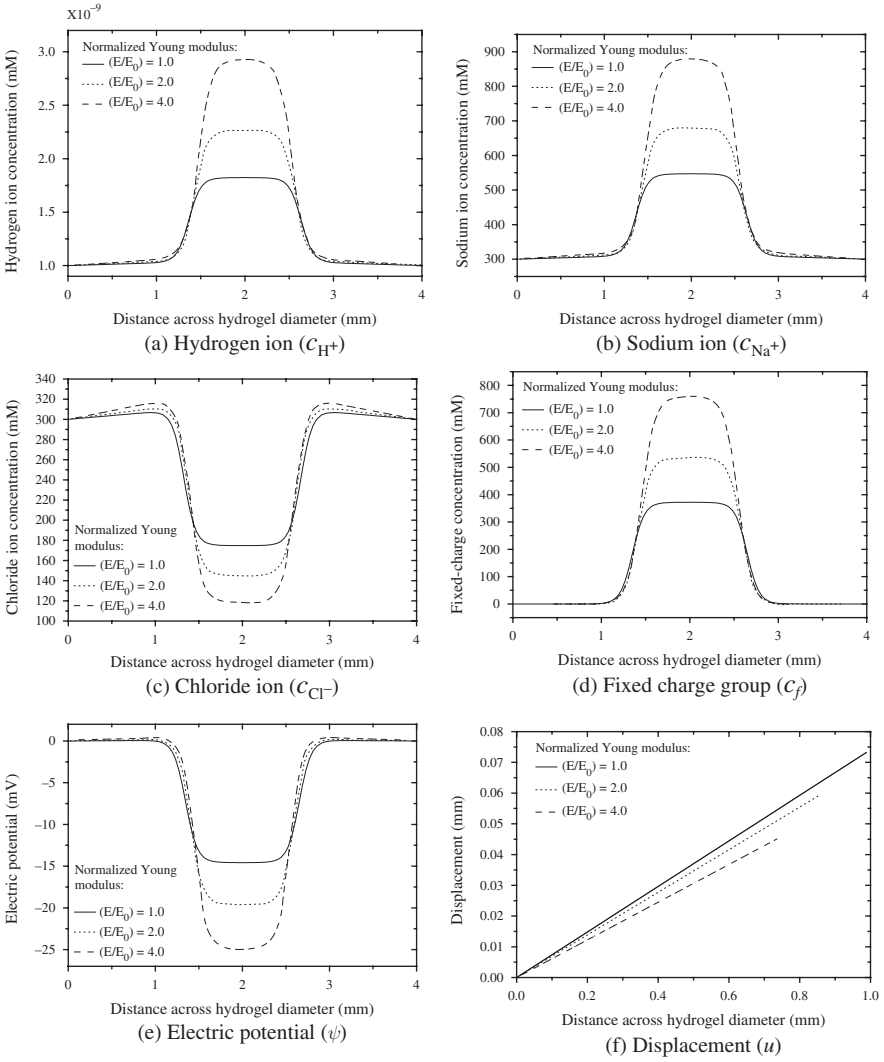

Fig. 2.12 Distributive profiles of c_{H^+},c_{Na^+},c_{Cl^-},c_f,ψ and u as the function of normalized Young's modulus (E/E_0), where the PHEMA hydrogel is equilibrated in basic medium of pH 12 with NaCl added to control the ionic strength

ratio of copolymer mixture which directly quantifies the density of entanglement strands or crosslinking ratio. As the crosslinking content increases in the polymer network, the hydrogel enhances larger retraction force and thus develops higher Young's modulus. The phenomenon always exists regardless of buffer contents as depicted in Fig. 2.14. The diameters of the swollen hydrogels are plotted against the normalized Young's modulus for the buffer solutions of pH 3 and 9. The increase of Young's modulus reduces exponentially the swelling of the hydrogels for the three

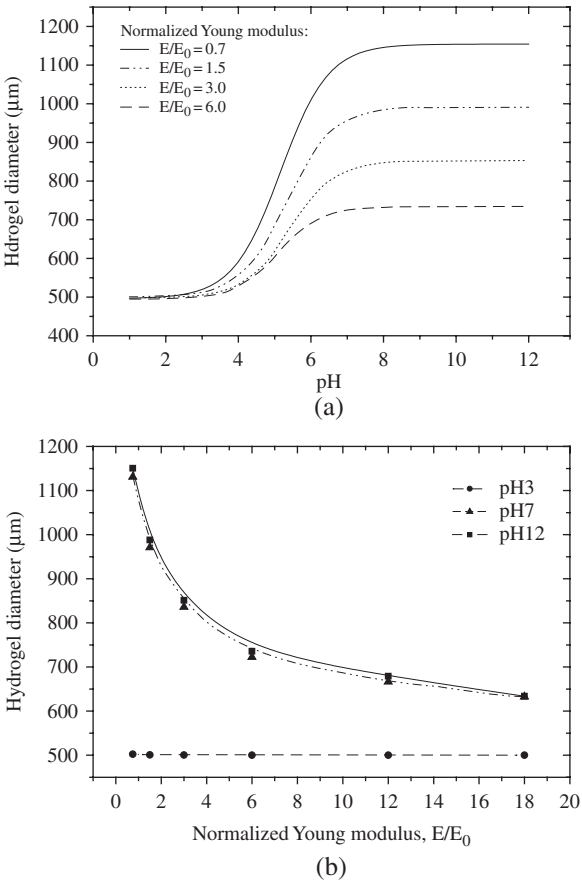

Fig. 2.13 Dependence of swelling on (**a**) bathing pH as the function of normalized Young's modulus (E/E_0) and (**b**) varying normalized Young's modulus (E/E_0) in acidic, neutral and basic solutions

different buffer systems as illustrated in Fig. 2.14. Influence of buffer contents on the swelling equilibrium at higher pH is more significant than that at lower pH. When the pH of buffer solutions is low, the degree of swelling of the hydrogel is almost insignificant even in different buffer systems and Young's moduli. If the pH is high, the obvious differences in the degree of swelling are observed for different buffer systems. Further, the Britton–Robinson is the unchanging leader for providing the better buffer solution when large swelling scale is required. It should be pointed out that the influence of the buffer contents vanishes if Young's modulus is high enough.

2.5.3 Influence of Initial Geometry of Hydrogel

Figures 2.15, 2.16 and 2.17 are plotted for the distributive profiles of the diffusive ionic concentrations and the electric potential as well as the mechanical displacement as function of the initial diameter of the hydrogel at the state before it is

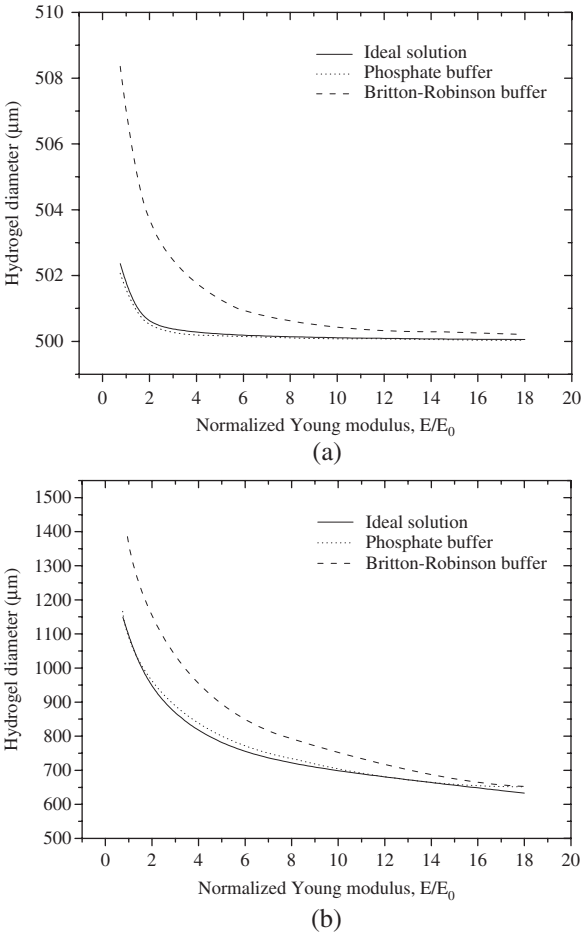

Fig. 2.14 Influences of buffer systems on swelling equilibrium as the function of normalized Young's modulus (E/E_0) in (**a**) acidic medium of pH 3 and (**b**) basic medium of pH 9

immersed in solution. The bathing solution is the electrolyte which is composed of NaCl and/or HCl. For the three pH buffered conditions, pH 3, 7 and 12, the concentrations of cations inside the hydrogel are higher, whereas those of anions are lower in comparison with those in the external solution. These are the performance expected because of the negative sign of the ionized charge groups dangling on the network matrix of the PHEMA hydrogel. Similarly, the electric potential exists as long as the migrations of ions occur between the interior hydrogel and the exterior solution.

Since both the hydration and fixed charge concentration kept almost constant against different initial geometries of the hydrogel as shown in Figs. 2.17 and 2.18, the swelling of the hydrogels behaves negligibly when they are soaked in electrolyte solution. The characteristics are found more clearly in Fig. 2.18, where the hydrations of the swollen hydrogels are plotted against the different pH levels

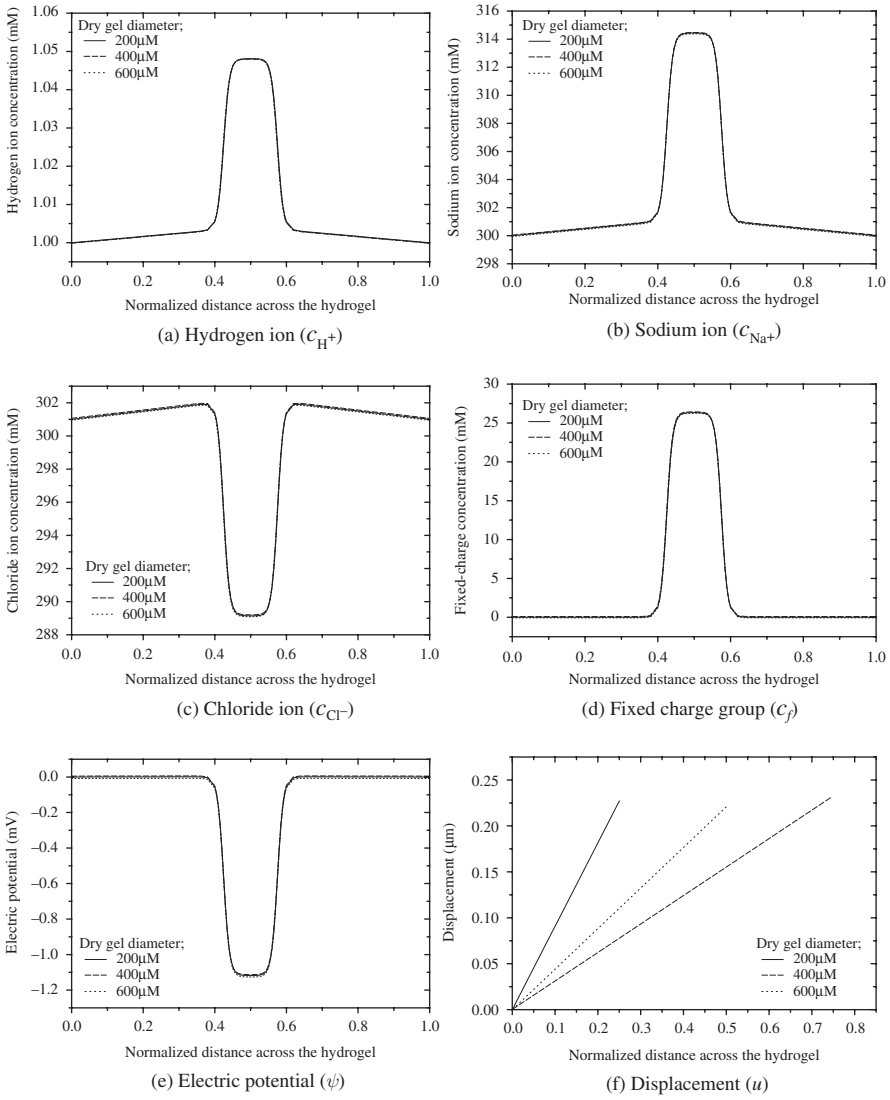

Fig. 2.15 Distributive profiles of c_{H^+},c_{Na^+},c_{Cl^-},c_f,ψ and u as the function of initial diameter of the dry gel, where the PHEMA hydrogel is equilibrated in an acidic medium of pH 3 with NaCl added to control the ionic strength

and dry gel diameters. As mentioned before, the diameters of dry gel are determined by the diameters of the nominal photomasks and the hydration is calculated by $H = V^f/V^s$.

In order to understand the responsive characteristics of the hydrogel bathed in different buffer solution systems, several simulations are carried out to predict the

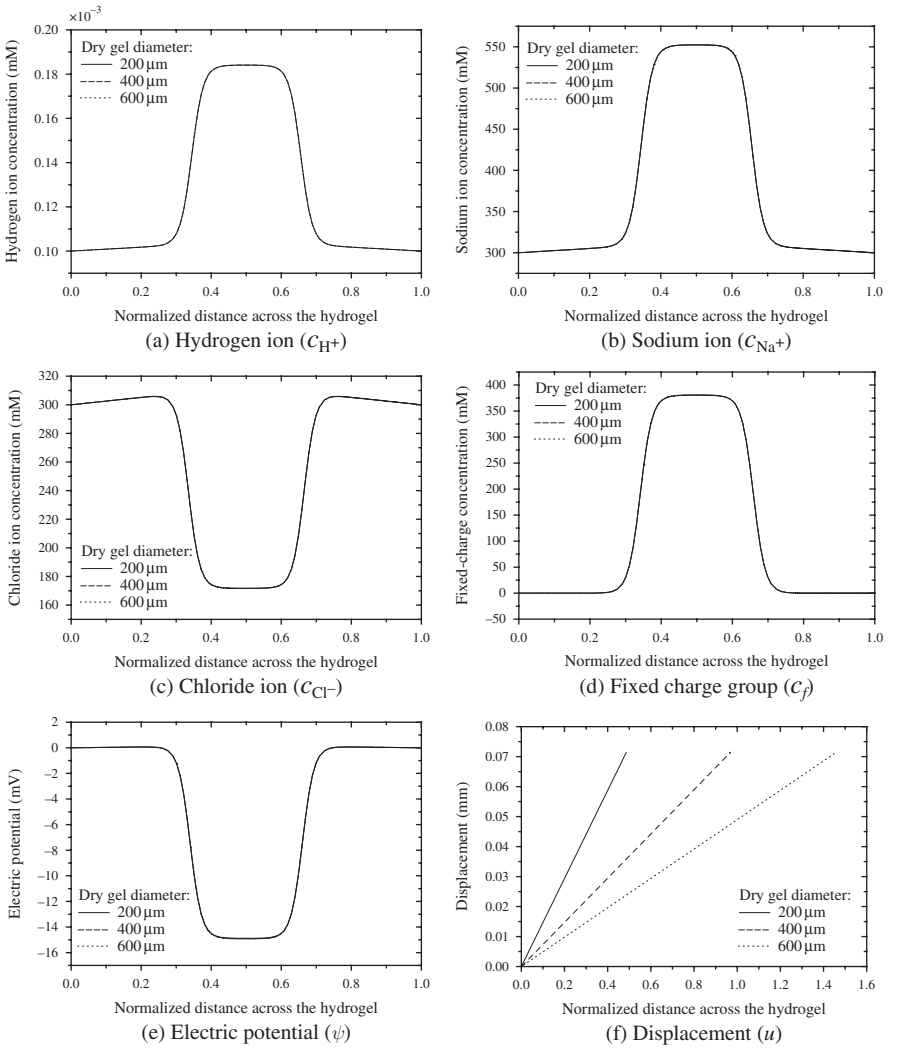

Fig. 2.16 Distributive profiles of c_{H^+},c_{Na^+},c_{Cl^-},c_f,ψ and u as the function of initial diameter of the dry gel, where the PHEMA hydrogel is equilibrated in a neutral medium with NaCl added to control the ionic strength

dilation of the hydrogels soaking in the phosphate buffer and Britton–Robinson buffer solutions. Figure 2.19 provides the comparison of swelling degree of the hydrated hydrogel for the three buffer solutions at pH 3 and 9 levels. The figure shows the significant independency of swelling on the initial diameters of the hydrogels. Similar to the previous discussions, the Britton–Robinson buffer always demonstrates a potentiality as buffer environment solution to meet the need of voluminous swelling.

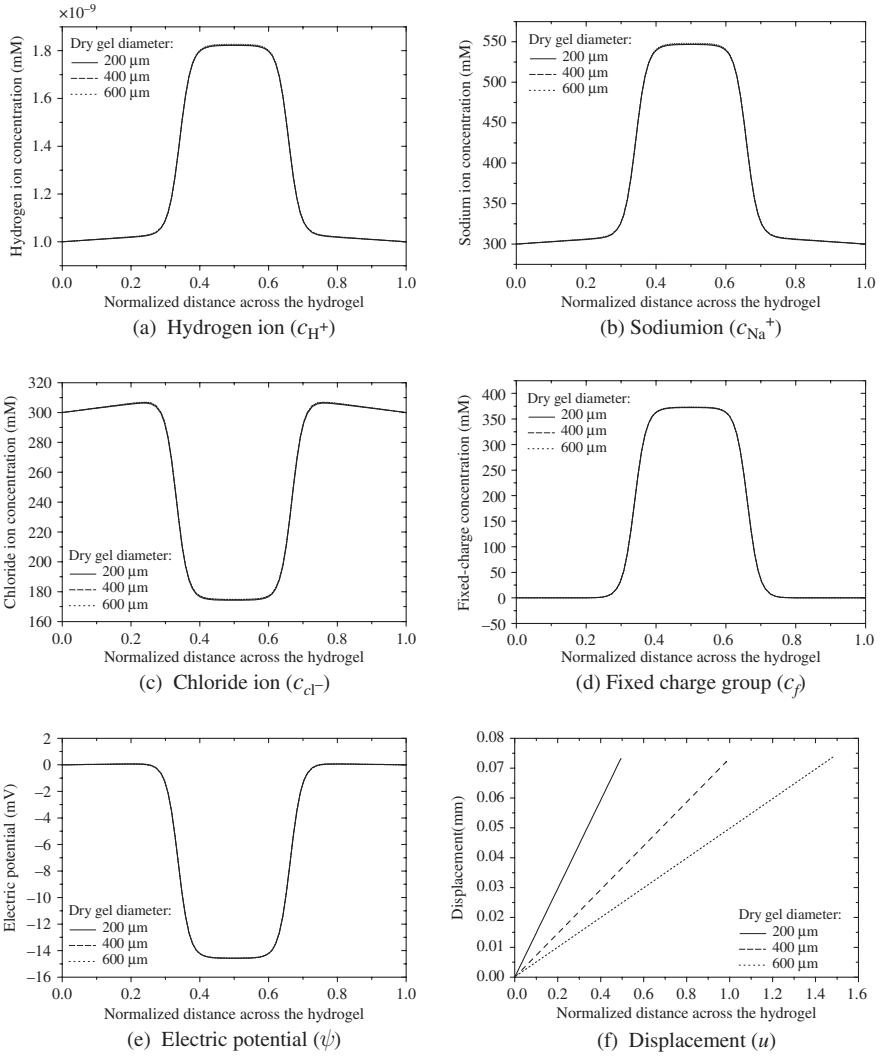

Fig. 2.17 Distributive profiles of c_{H^+},c_{Na^+},c_{Cl^-},c_f,ψ and u as the function of initial diameter of the dry gel, where the PHEMA hydrogel is equilibrated in a basic medium of pH 12 with NaCl added to control the ionic strength

2.5.4 Influence of Ionic Strength of Bath Solution

Figures 2.20, 2.21 and 2.22 are plotted to investigate the characteristics of diffusive ionic species, electrical potential and mechanical deformation of the pH-responsive hydrogel as function of environmental ionic strength conditioning.

It is widely accepted that the osmotic pressure arises from the concentration difference between the interior hydrogel and the external solution, and the swelling of

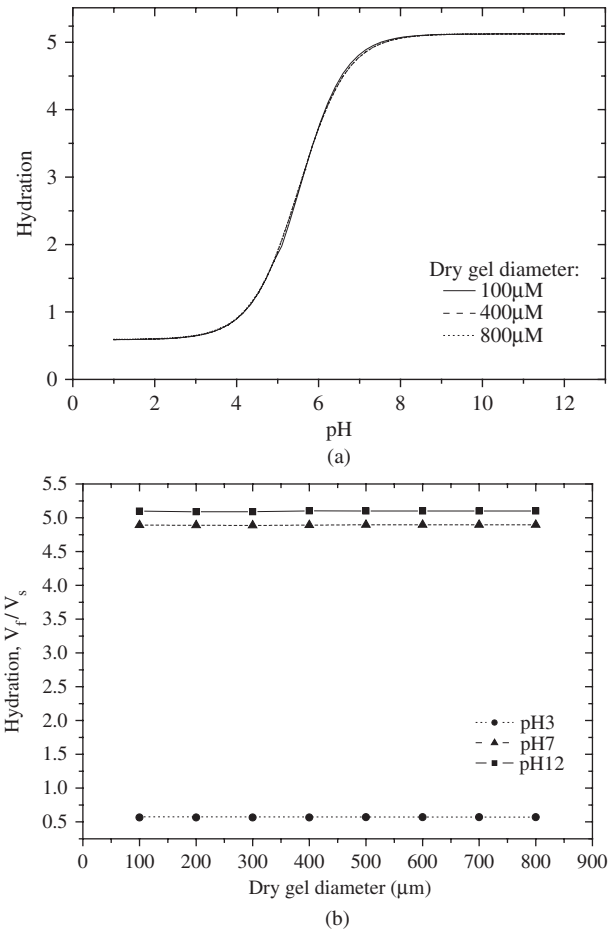

Fig. 2.18 Dependence of hydration on (**a**) bathing pH as the function of initial diameter of the dry gel and (**b**) the diameter of the dry gel in acidic, neutral and basic solutions

the hydrogel in equilibrium can be approximated by examination of the concentration ratio between the interior and exterior of the hydrogel, which is coherent with the definition of Donnan equilibrium (Flory, 1962; Helfferich, 1962). The osmotic pressure is usually regarded as outward pressure in excess of the pressure of surrounding solution, which would result in expanding of the polymer network. In order to discuss the problems with different bath solution concentrations, it is convenient to introduce the density ratio or better known as Donnan ratio λ_D as follows (Ricka and Tanaka, 1984; Siegel, 1990; Homma et al., 2000):

$$\lambda_D = \left(\frac{c_k}{\bar{c}_k}\right)^{1/z_k} \tag{2.60}$$

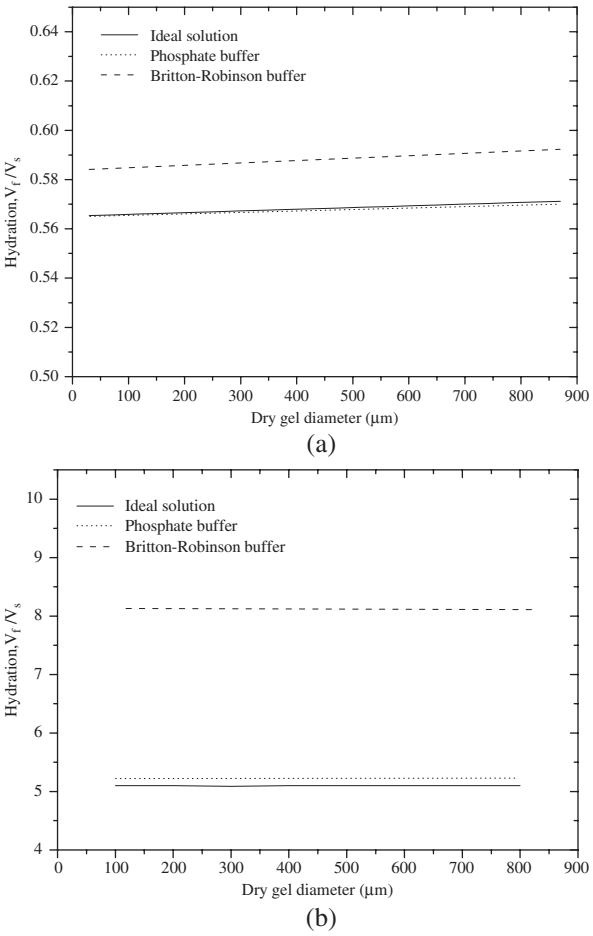

Fig. 2.19 Influences of buffer systems on hydration as the function of initial diameter of the dry gel in (**a**) acidic medium of pH 3 and (**b**) basic medium of pH 9

where z_k, c_k and $\bar{c}_k$ ($k = 1,2,3,...,N_{\text{ion}}$) are the valence number and the concentrations in the hydrogel and the external solution for the kth diffusive ion species, respectively. As the concentrations of the external solution keep constant everywhere in equilibrium sate, $\bar{c}_k$ are allowed to take the concentration boundary values of corresponding ionic species.

The distributions of the concentrations of diffusive Na^+ and Cl^- species are presented in the form of Donnan ratio and shown in Fig. 2.20. It is evident that the mobile cations, hydrogen (H^+) and sodium (Na^+) ions, have higher concentrations within the interior hydrogel than those in the exterior solution, while the mobile anions, chloride (Cl^-) ion, show a contrary pattern. However, the requirement of electroneutrality condition is always met everywhere in the domain of surrounding solution.

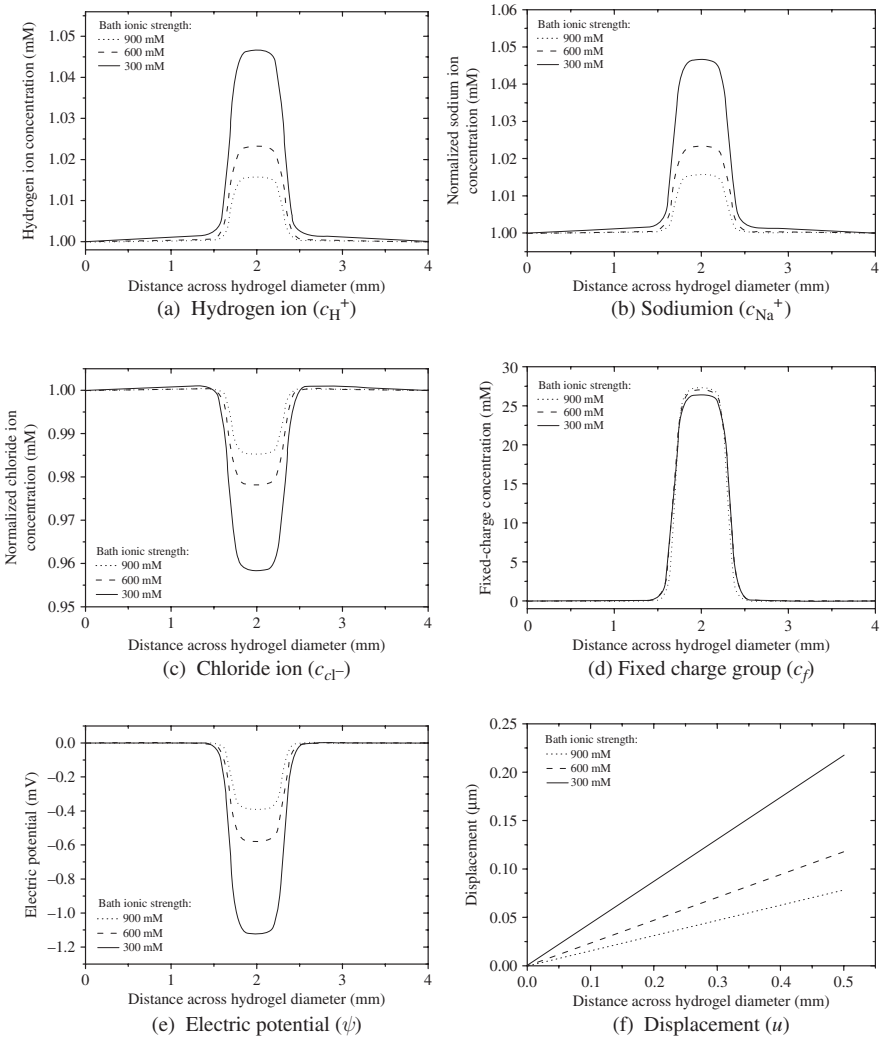

Fig. 2.20 Distributive profiles of c_{H^+},c_{Na^+},c_{Cl^-},c_f,ψ and u as the function of the ionic strength of medium, where the PHEMA hydrogel is equilibrated in acidic medium of pH 3 with NaCl added to control the ionic strength

As the ionic strength of bath solution increases, the ratio of the ionic concentrations decreases between the interior hydrogel and the exterior bath solution (Siegel, 1990). On this account, the osmotic pressure becomes less and the reduction of the hydration is expected. The fixed charge density is a function of the hydration of the swollen hydrogel, the total ionizable groups per volume of network polymer and the concentration of diffusive H^+ ion provided by the outer solution. Since the increases of the ionic strength is controlled by NaCl, the totally resultant concentration of

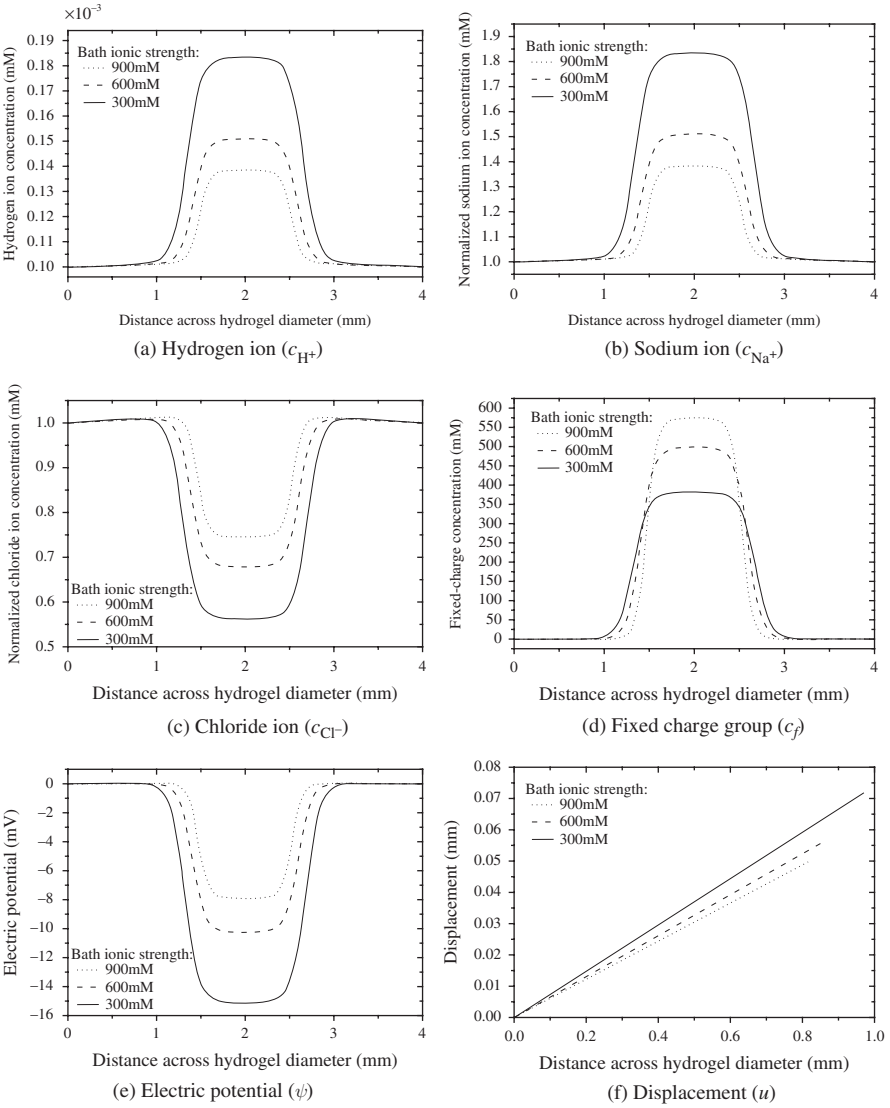

Fig. 2.21 Distributive profiles of c_{H^+},c_{Na^+},c_{Cl^-},c_f,ψ and u as the function of the ionic strength of medium, where the PHEMA hydrogel is equilibrated in neutral medium with NaCl added to control the ionic strength

H^+ ion and ionizable groups remains constant. Therefore, it is foreseeable that the redistribution of the fixed charge concentration is controlled mainly by the hydration. Due to the change of the fixed charge concentrations, there are the concurrent changes in the concentration profiles of the diffusive cations and anions. The interaction continues until new equilibrium state is achieved. The phenomena become more obvious at higher solution pH, as seen in Figs. 2.21 and 2.22.

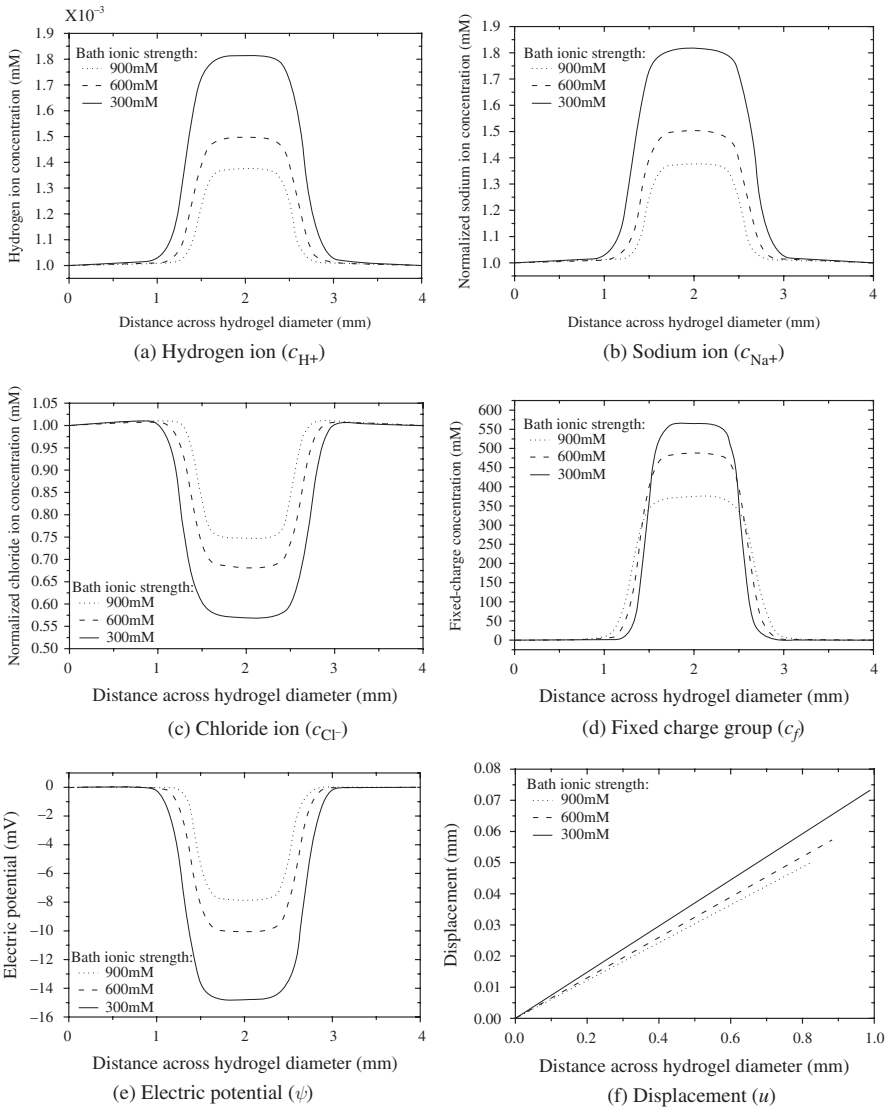

Fig. 2.22 Distributive profiles of c_{H^+},c_{Na^+},c_{Cl^-},c_f,ψ and u as the function of the ionic strength of medium, where the PHEMA hydrogel is equilibrated in basic medium of pH 12 with NaCl added to control the ionic strength

Figure 2.23a, b theoretically demonstrates the influences of the ionic strength of bathing solution on the equilibrium swelling of the HEMA hydrogel with the identical fixed charge density and Young's modulus. As predicted, the hydrogel behaves like a hydrophobic polymer network at low pH. After pH 4, however, the fluid phase content within the hydrogel increases abruptly and thus results in highly

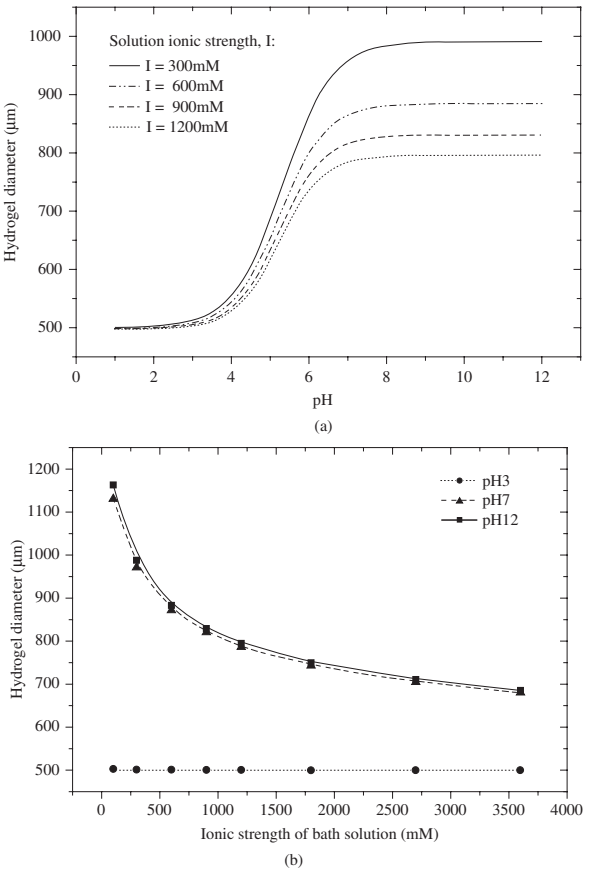

Fig. 2.23 Dependence of swelling on (**a**) bathing pH as the function of ionic strength of bath medium and (**b**) varying ionic strengths in acidic, neutral and basic mediums

swollen hydrogel. Apart from that, the highest curve is associated with the solution for the ionic strength of 300 mM, while subsequently lower curves correspond to the bath solutions with higher ionic strength, increasing regularly from 600 to 1200 mM. In the surrounding solutions with very low ionic strengths, the hydrogen (H^+) ions play an essential role in association or dissociation process. This implies that the contributions of other mobile ion species to the osmotic pressure are minimized. However, as the ionic strength of bathing solution increases, the degree of swelling decreases for high ambient pH. This phenomenon is in accordance with the experimental observation by Siegel and his team (1988, 1990, 1991).

Figure 2.24 focuses on the dependence of equilibrium swelling on the ionic strength of certain buffer systems, where two diverse solutions are considered for comparison and they are the NaCl/HCl solution and the phosphate buffer solution with a calculated amount of NaCl added to adjust the ionic strength at a desired level. The responsive characteristics of the pH-sensitive hydrogel perform exponentially the decrease of the degree of swelling as the environmental ionic strength

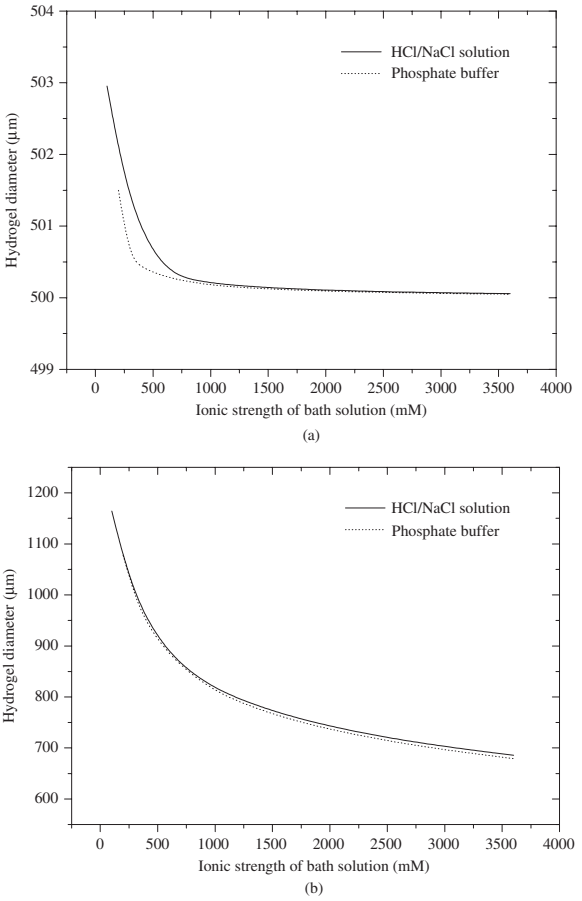

Fig. 2.24 Influences of buffer systems on hydration as the function of ionic strength of bath medium in (**a**) acidic medium of pH 3 and (**b**) basic medium of pH 9

increases for both the bathing solutions. The observations are comparable with the experimental work by Brannon-Peppas and Peppas (1991). Insignificant difference of swelling is found for both the solutions. In all likelihood, both the solutions do not make enormous difference as the dominant counterions are essentially the univalent ions which are mainly the sodium ions (Siegel et al., 1991).

2.5.5 Influence of Multivalent Ionic Composition of Bath Solution

In order to investigate the influences of multivalent ionic compositions of bath solutions on the equilibrium swelling, the multivalent polyelectrolyte solution is considered in this section. Influences of bath compositions with multivalent ions on the characteristics of pH-dependent equilibrium swelling are shown in

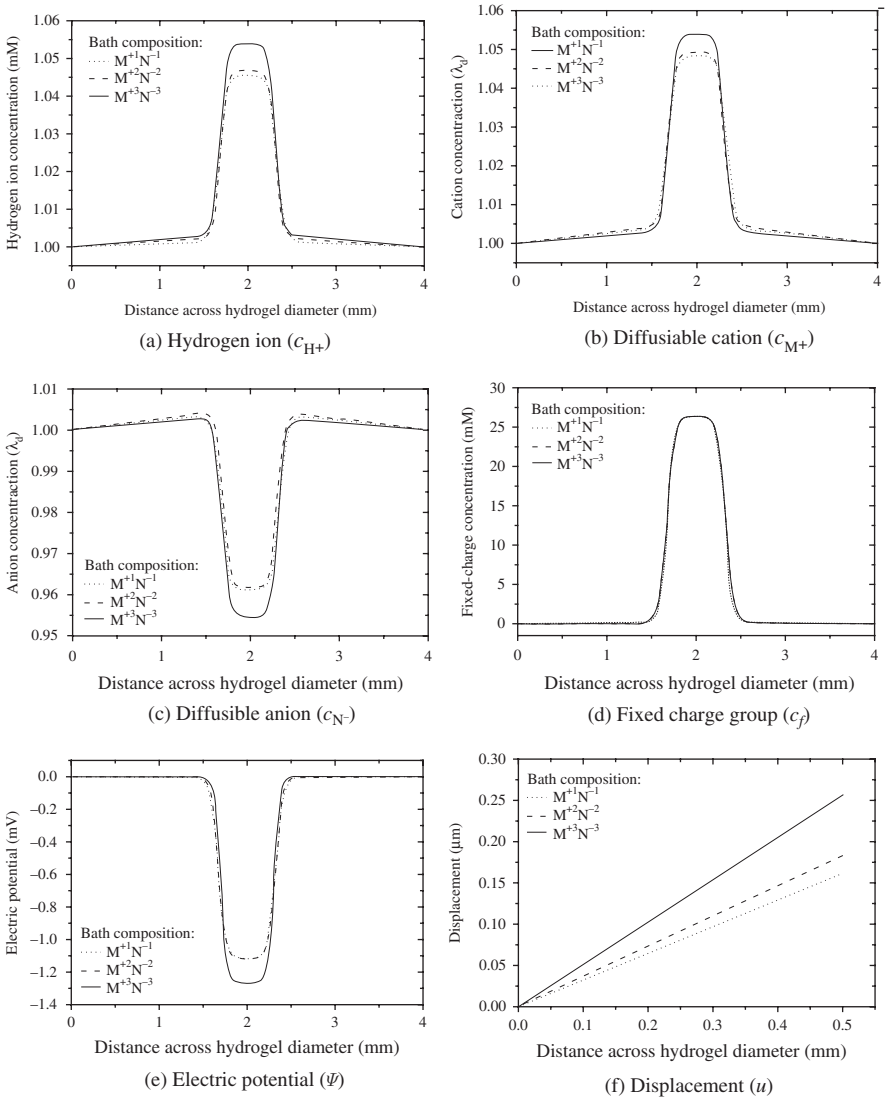

Fig. 2.25 Distributive profiles of c_{H^+},c_{M^+},c_{N^-},c_f,ψ and u for specified solvent composition (monovalent, divalent and trivalent), where the PHEMA hydrogel is equilibrated in acidic medium of pH 3

Figs. 2.25, 2.26, 2.27, 2.28 and 2.29, where the relevant conditions are maintained at the temperature of 25°C and the ionic strength of 300 mM. For analysis of the characteristics of the hydrogel swelling, the bathing solution is assumed reasonably to be primarily composed of symmetrical salt (z:z) with varying ionic valences, namely $M^{+1}N^{-1}$, $M^{+2}N^{-2}$ and $M^{+3}N^{-3}$.

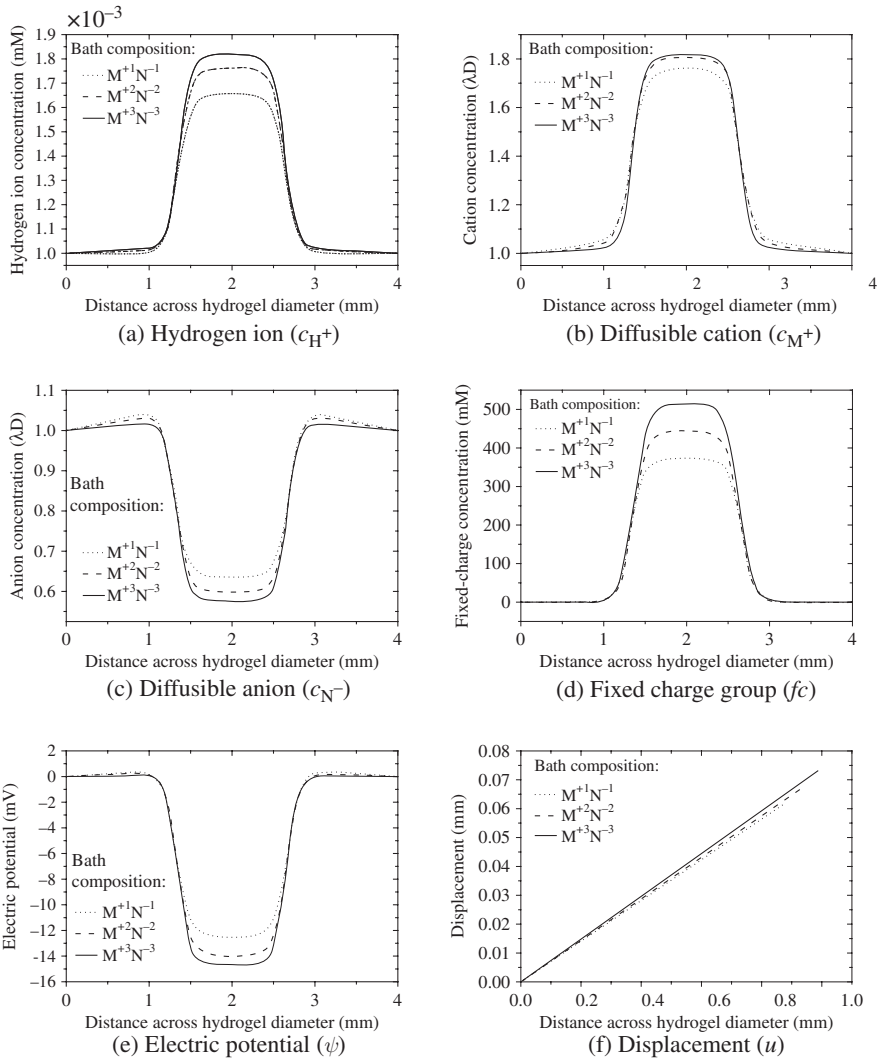

Fig. 2.26 Distributive profiles of c_{H^+},c_{M^+},c_{N^-},c_f,ψ and u for specified solvent composition (monovalent, divalent and trivalent), where the PHEMA hydrogel is equilibrated in a neutral medium

Figures 2.25, 2.26 and 2.27 demonstrate the concentration profiles of mobile ion species and fixed charge groups, and the profiles of electric potential and mechanical displacement predicted in equilibrium. The Donnan concentrations of the sodium and chloride ions are presented for the sake of apprehensible comparison of the osmotic pressure. When the profiles of the ionic concentrations are determined, Donnan ratio λ_D becomes an elegant tool for estimating quantitatively the

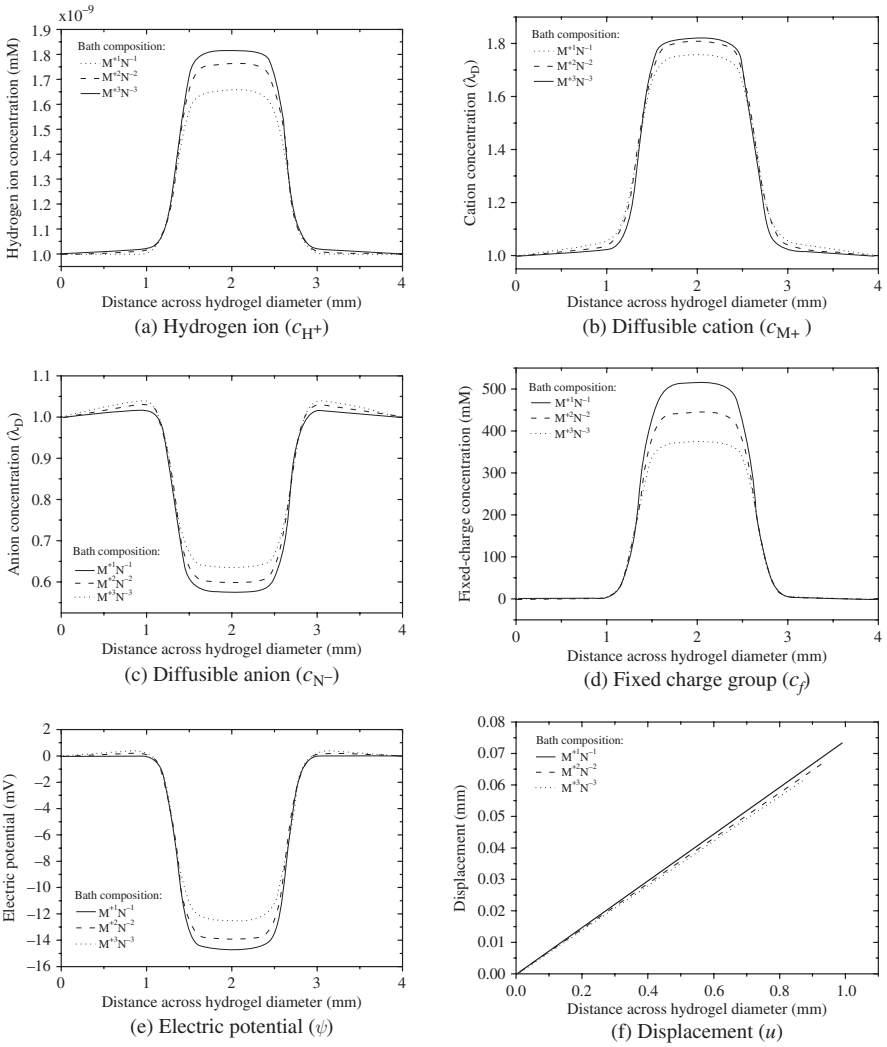

Fig. 2.27 Distributive profiles of c_{H^+},c_{M^+},c_{N^-},c_f,ψ and u for specified solvent composition (monovalent, divalent and trivalent), where the PHEMA hydrogel is equilibrated in basic medium of pH 12

swelling of the hydrogel, if the influence of bath composition is studied with different ion valences and ionic strengths. Discrepancies in the profiles and the degrees of swelling are insignificant for acidic solution, as observed from Fig. 2.25. However, they show the trend similar to those for the cases with neutral and base solutions, as shown in Figs. 2.26 and 2.27. Specifically, the Donnan ratio λ_D or the concentrations of mobile ions within the hydrogel decreases as the ionic valence increases, and consequently the equilibrium swelling reduces as predicted. The distribution

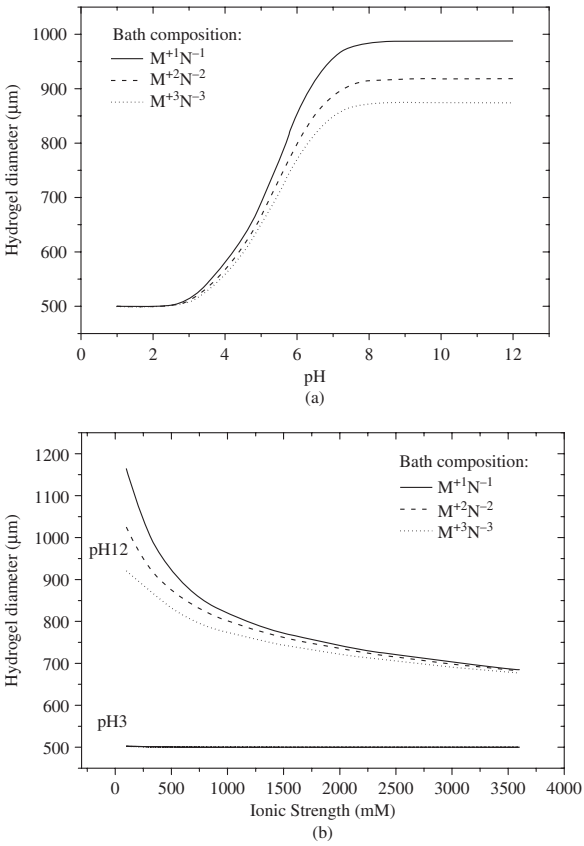

Fig. 2.28 Dependence of swelling on (**a**) solvent composition (monovalent, divalent and trivalent) as the function of bathing pH and (**b**) ionic strength of bath medium with different ionic valences

of the fixed charge concentration in Fig. 2.25d seems to be the same for all conditions, but actually the values of the concentrations are different from each other, namely 26.41631 mM for $M^{+3}N^{-3}$, 26.39451 mM for $M^{+2}N^{-2}$ and 26.38594 mM for $M^{+1}N^{-1}$. Therefore, the ionized groups attached on the hydrogel network tend to increase as the ionic valences of the solution increase due to the reduction of equilibrium swelling.

Figure 2.28a, b exhibits the influences of the ionic valences on the responsive equilibrium swelling of an acidic hydrogel at certain pH levels. It is seen that the solvent composition strongly influences the characteristics of swelling. This is consistent with the published experimental works (Siegel and Firestone, 1988; Siegel, 1990), in which as the salt (solvent) valence of the solution increases, the ion osmotic effect is expected to decrease significantly, because less amount of counterions diffuse into the hydrogel for neutralization of the charged groups. All the present discussions make the simulations in agreement with the experiment and they are also found in Fig. 2.28a, b, from which it is clearly known that the response of the hydrogel immersed in the solution with the larger ionic valence behaves the smaller deformation of the hydrogel. The effects of multivalent ionic composition of bath solution gradually fade out as the ionic concentration increases.

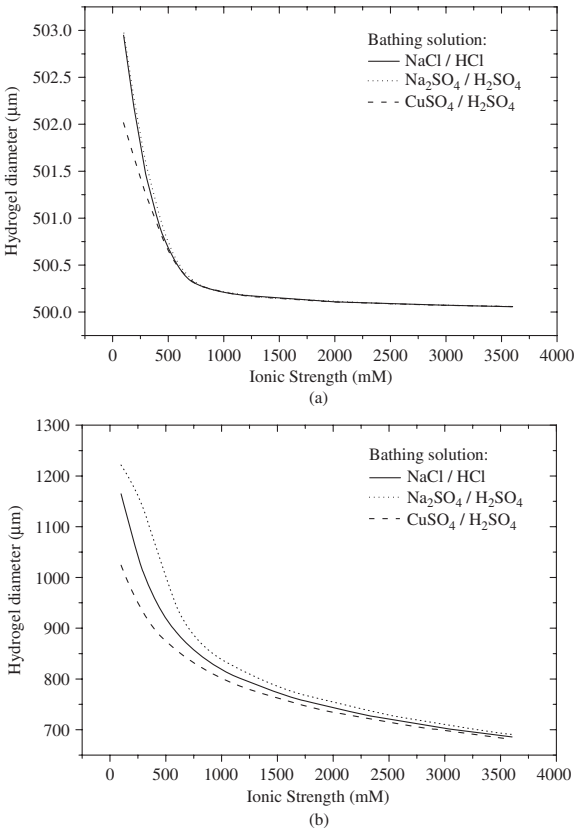

Fig. 2.29 Effects of ionic valences of bathing solution on swelling equilibrium as the function of ionic strength in (**a**) acidic medium of pH 3 and (**b**) basic medium of pH 9

A further comparison study is made between an asymmetrical salt (Na_2SO_4) solution and a symmetrical salt (NaCl and $CuSO_4$) solution, and demonstrated in Fig. 2.29 for both the acidic pH 3 and basic pH 9 mediums. The degree of changes in equilibrium swelling of the hydrogel in Na_2SO_4 solution is higher than that in NaCl for base environment, even though the counterion species is identical. This may be explained by the difference of the sodium ion (counterion) concentrations in the two bathing solutions. In order to maintain the electroneutrality and the ionic strength, the sodium ion concentration in Na_2SO_4 electrolyte solution is at a lower level. As a result, the pressure gradient between the interior hydrogel and the exterior solution tends to increase, leading to larger amount of swelling. On the contrary, the $CuSO_4$ solution shows the lowest degree of swelling. Since fewer divalent and monovalent counterions are required to neutralize the carboxylic acid groups, this causes relatively low concentration gradient and thus reduces the equilibrium swelling. On the other hand, the differences in the degree of swelling are insignificant until the ionic strength decreases below 600 mM as shown Fig. 2.29a. Therefore, the ionic valences still play some part in the mechanism of swelling but a secondary role as compared with the pH condition and ionic strength of the bathing solution (Siegel and

Firestone, 1988). The extent of swelling increases exponentially with the decrease of the ionic strength regardless of the bath contents at high pH. However, the asymmetrical electrolyte solution shows the inclination of swelling at low ionic strength with high pH.

2.6 Remarks

The modulating capability of absorbing or exuding the fluid for the smart hydrogel stimulated by surrounding environmental pH enables us to dynamically control the swelling/deswelling, and thereby achieve the effective diffusibility and permeability of the solutes and mechanical energy in the hydrogel. In addition, the presence of the electrostatic potential that is locally induced in the electrolytic solution by movement of all diffusive ionic species is an important phenomenon occurring in an ionic diffusion, but not in non-electrolyte species diffusion. In the ionic solution, the local electroneutrality is conserved everywhere. During the diffusion, all ions do not move at the same speed because different ionic species tend to diffuse at different rates. However, excessive charges contributed by the faster ions build up a local electric field, also called the diffusion potential, which slows down the faster ions and reciprocally accelerates the slower ionic species. Further, the diffusion potential should also be considered even if an external electrical field is applied to the system, by superimposing the diffusion potential upon the externally applied electrical field, as shown in Fig. 2.30.

The interactions between the hydrogel elastic polymer network and chemical medium strongly influence the degree of responsive swelling/deswelling of the smart hydrogel. The ionizable polymer fractions in the hydrogel are capable of associating and dissociating themselves, which characterizes the physicochemical properties of the hydrogels. When the hydrogel is immersed in a buffered solution, the electrolytic composition of the surrounding solution diffuses into the hydrogel and this determines the dissociation or association of the polyelectrolyte fraction of the hydrogels. Chemical reactions occur as a result of the reversible process of dissociation/association between the diffusive mobile ions and the ionizable groups attached on the hydrogel network, and subsequently redistribute the ionic concentrations within the hydrogel. The redistributions of ionic concentrations within the hydrogel generate both the electrostatic field and the osmotic pressure due to the difference of ionic concentrations between the hydrogel and surrounding environment. The osmotic pressure drives the expansion or contraction of the hydrogel. The swelling or shrinking subsequently redistributes the ion concentration of the interior hydrogel. The loop continues until equilibrium is achieved.

In this chapter, the formulated electrochemical and mechanical equations that are coupled together through the hydration are known collectively as the multi-effect-coupling pH-stimulus (MECpH) model for simulation of the responsive characteristics of the multiphase pH-sensitive hydrogel and surrounding solution. The MECpH model does have the following advantages that make this model more attractive than other models in certain aspects.

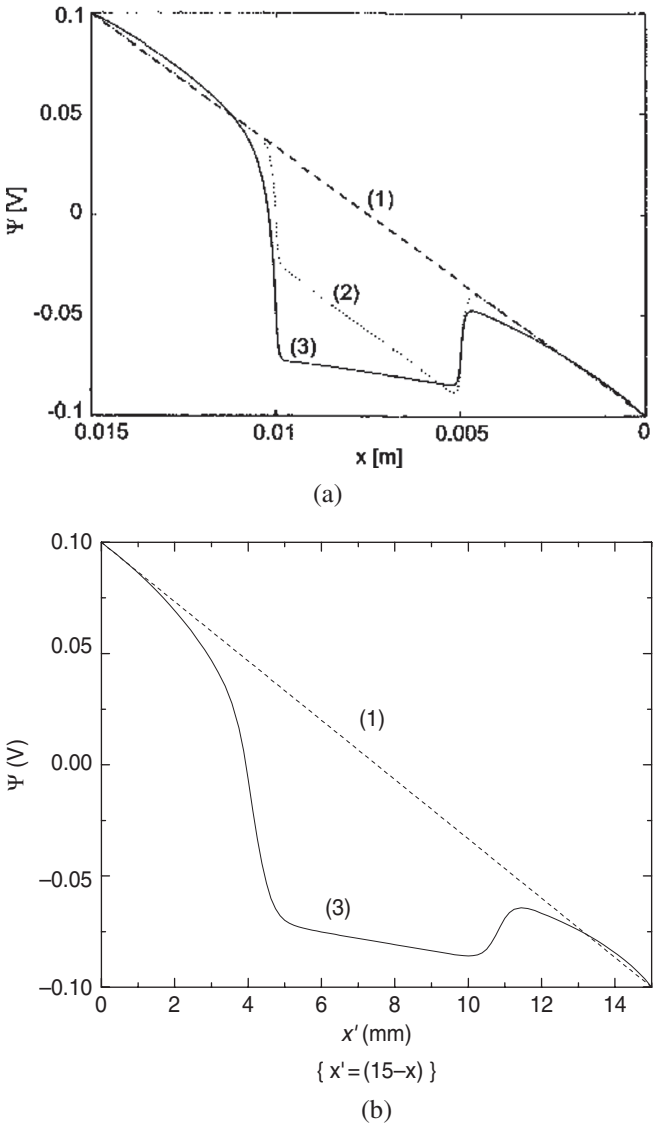

Fig. 2.30 Comparison of electrical potential in the hydrogel and bathing solution due to externally applied electric field between (**a**) stabilized space–time FEM (Wallmersperger, 2001a) and (**b**) Hermite-cloud meshless methods (Li et al., 2003)

- Computational domains of interest cover both the interior hydrogel and the exterior bathing solution. The model is thus able to predict the distributions of concentrations of all diffusive species, electric potential in both the hydrogel and surrounding solution simultaneously.

- MacGillivary (1968) pointed out that the electroneutrality and constant field assumptions are in fact nothing new but two limited cases of a dimensionless parameter, which is associated with the ratio of the Debye length to membrane thickness. The Poisson equation provides a more robust approach to account for the effect of electrical potential coupled with various ionic fluxes.
- Theoretically, the distribution of the fixed charge density is a function of the material properties and hydration of the hydrogel. In the MECpH model, the Langmuir adsorption isotherm is introduced to derive the fixed charge concentration, expressed by a function of the hydration, the diffusive hydrogen ion H^+ concentration and the concentration of fixed charge groups per polymer network volume.
- The MECpH model can easily handle the large deformation of the pH-sensitive hydrogels, based on the geometrically nonlinear finite deformation theory. This is another advantage of the model since the pH-sensitive hydrogels usually undergo very large displacement due to the chemo-electro-mechanical multi-energy coupled effects, especially at higher pH levels of environmental solutions.
- The MECpH model can also easily incorporate multiple ionic species, unlike other models where only two monovalent ion species, an anion and a cation, are considered.
- The MECpH model is formulated in very elegant form, in which several key effects on the responsive behaviours of the pH-sensitive hydrogel and surrounding solution are expressed in a straightforward manner. The model is readily applicable for numerical implementation as compared with other models.

We believe that the pH-sensitive hydrogel, like ionic exchanger found in natural charged membranes, contains substantial ionizable groups capable of dissociating and subsequently achieving net charge due to buffered medium. These groups are capable of ionizing as a function of the electrolyte pH and the ionic strength and thereby producing positive or negative charges fixed onto the polymeric network chains.

The pendent charges fixed on the backbone of the polymer network of the hydrogels, e.g. carboxylic group, exist in the form of $R–COO^-$ in basic solution and in the form of R–COOH in acid medium as mentioned above. When the pH of surrounding medium is higher than the pK_a of the weakly acid group bound to the polymeric network, the chemical reactions proceed to the forward direction. As a result, the hydrogel achieves higher fixed charge density. In order to maintain the electroneutrality within the hydrogel, more mobile counterions (e.g. Na^+if the sodium chloride electrolyte solution is added to adjust the ionic strength) diffuse into the interior hydrogel to compensate the surplus charges. In vice versa, the mobile ions with the same sign of the fixed charge groups are repulsed from entering the interior hydrogel. However, besides those compensating counterions, there are also the absorbed counterions which are accompanied by equivalent amount of co-ions (Helfferich, 1962). By understanding of the mechanism of the distributive ionic concentrations in the interior hydrogel, it is clearly known that the concentration of the Na^+ ion is

higher whereas that of Cl^- ion is lower for alkaline solution if compared with acidic solution.

The uptake or sorption of mobile ions essentially redistributes the mobile ions between the two liquid states, the interstitial liquid phase within the hydrogel and the bathing solution, until equilibrium is attained. As a result, the concentration difference increases tremendously between the interior hydrogel and the exterior solution, leading to higher osmotic pressure which drives larger degree of swelling. In the meantime, the elastic retractive force of the polymer network balances with the expanding network. The interacting process carries on forward and backward until equilibrium state is achieved.

Theoretical simulation reveals that the swelling behaviour of the HEMA hydrogels may be divided into three states: (1) the insignificant swelling because of the compact and hydrophobic states at pH values lower than 4 regardless of monomer composition, (2) the ionization takes place actively if the pH ranges from 4 to 7 where the fluid content within the hydrogels increases abruptly and gives rise to highly swollen hydrogel and (3) the binding sites of charge groups are saturated at environmental pH higher than pH 7 and the hydrogels do not further expand significantly even the surrounding pH increases continuously.

There are also secondary parameters influencing the expansion and contraction of the charged crosslinked hydrogels. In addition to the pH sensitivity, swelling and deswelling are also dependent on physical and chemical properties of the smart hydrogel as well as the ionic strength and composition of surrounding medium. These observations are all consistent with experimental phenomena reported in open literature.

Similar phenomena are observed for analysis of response characteristics of ionic species and electrical potential when the smart hydrogel is exposed to the phosphate and Britton−Robinson buffer systems, as compared with HCl/NaCl solution. Quantitatively, the degree of swelling is almost the same between the phosphate buffer and HCl/NaCl solution, where the pH-sensitive hydrogel is placed. In another study, the equilibrium swelling of the smart hydrogel in the Britton–Robinson buffer solution is predicted to be always larger than that bathed in the phosphate buffer system and HCl/NaCl solution. Probably one of the reasons is that the Britton–Robinson buffer system has lower ionic strength than those of the phosphate buffer system and HCl/NaCl solution. However, the identity of buffer ions may also play an important role.

References

D.J. Beebe, J.S. Moore, J.M. Bauer, Q. Yu, R.H. Liu, C. Devadoss, B.H. Jo. (2000a). Functional hydrogel structures for autonomous flow control inside microfluidic channels. *Nature*, 404, 588–590.

D.J. Beebe, J.S. Moore, Q. Yu, H. Liu, M.L. Kraft, B.H. Jo, C. Devadoss. (2000b). Microfluidic tectonics: A comprehensive construction platform for microfluidic systems. *Proceedings of the National Academy of Sciences of the United States of America*, 97, 13488–13493.

J.O'M. Bockris, B.E. Conway, E. Yeager (Eds.) (1983). *Comprehensive Treatise of Electrochemistry*, Vol. 6, *Electrodics: Transport*, New York: Plenum Press.

J.O.M. Bockris, K.N. Reddy-Amulya. (1998). *Modern Electrochemistry: Ionics*, 2nd edn. New York: Plenum Press.

L. Brannon-Peppas, N.L. Peppas, (1991). Equilibrium swelling behavior of pH-sensitive hydrogels. *Chemical Engineering Science*, 46, 715–722.

H. Brondsted, J. Kopecek. (1992). pH-Sensitive Hydrogels: Characteristics and Potential in Drug Delivery. In: *Polyelectrolyte Gels: Properties Preparation and Applications*, ACS Symposium Series 480, R.S. Harland, R.K. Prud'homme (Eds.) Washington DC: American Chemical Society, pp. 285–304.

L.D. Carnay, I. Tasaki. (1971). Ion Exchange Properties and Excitability of the Squid Giant Axon. In: *Biophysics and Physiology of Excitable Membranes*, W.J. Adelman Jr. (Ed.) New York: Van Nostrand Reinhold Co, pp. 379–422.

Y. Chu, P.P. Varanasi, M.J. McGlade, S. Varanasi. (1995). pH-induced swelling kinetics of polyelectrolyte hydrogels. *Journal of Applied Polymer Science*, 58, 2161–2176.

K. Cooper, E. Jakobsson, P. Wolynes. (1985). The Theory of ion transport through membrane channels. *Progress in Biophysics and Molecular Biology*, 46, 51–96.

E.L. Cussler. (1997). *Diffusion Mass Transfer in Fluid System*, 2nd edn. Cambridge: Cambridge University Press.

D. De Rossi, P. Parrini, P. Chiarelli, G. Buzzigoli. (1985). Electrically induced contractile phenomena in charged polymer networks: Preliminary study on the feasibility of muscle-like structures. *Transactions of the American Society for Artificial Internal Organs*, XXXI, 60–65.

M. Doi, M. Matsumoto, Y. Hirose. (1992). Deformation of ionic polymer gels by electric fields. *Macromolecules*, 25, 5504–5511.

L. Dresner. (1972). Some remarks on the integration of extended Nernst–Planck equations in the hyperfiltration of multicomponent solution. *Desalination*, 10, 27–46.

R.S. Eisenberg. (1999). From structure to function in open ionic channel. *Journal of Membrane Biology*, 171, 1–24.

P.J. Flory. (1953). *Principles of Polymer Chemistry*, Ithaca, New York: Cornell University Press.

A. Fragala, J. Enos, A. LaConti, J. Boyack. (1972). Electrochemical activation of a synthetic artificial muscle membrane. *Electrochimica Acta*, 17, 1507–1522.

S.H. Gehrke, E.L. Cussler. (1989). Mass transfer in pH-sensitive hydrogels. *Chemical Engineering Science*, 44, 559–566.

D. Gillespie, R.S. Eisenberg. (2001). Modified Donnan potentials for ion transport through biological ion channels. *Physical Review E*, 63, 061902.

D. Gillespie, R.S. Eisenberg. (2002). Physical descriptions of experimental selectivity measurements in ion channels. *European Biophysics Journal*, 31, 454–466.

D.E. Goldman. (1943). Potential, impedance and rectification in membranes. *Journal of General Physiology*, 27, 37–60.

D.E. Goldman. (1971). Excitability Models. In: *Biophysics and Physiology of Excitable Membranes*, W.J. Adelman Jr. (Ed.) New York: Van Nostrand Reinhold Co, pp. 337–358.

P.E. Grimshaw. (1989). Electrical control of solute transport across polyelectrolyte membranes. Ph.D Thesis, Massachusetts Institute of Technology.

P.E. Grimshaw, J.H. Nussbaum, A.J. Grodzinsky. (1990). Kinetics of electricity and chemically induced swelling in polyelectrolyte gels. *Journal of Chemical Physics*, 93, 4462–4472.

A.J. Grodzinsky. (1974). Electromechanics of deformable polyelectrolyte membranes. Sc.D Thesis, Massachusetts Institute of Technology.

R.W. Gulch, J. Holdenried, A. Weible, T. Wallmersperger, B. Kroplin. (2000). Polyelectrolyte Gels in Electric Fields: A Theoretical and Experimental Approach. In: *Smart Structures and Materials 2000: Electroactive Polymer Actuators and Devices, Proceedings of the SPIE 3987*, Y. Bar-Cohen (Ed.) Bellingham, Washington: SPIE Press, pp. 193–202.

L. Guldbrand, B. Jonsson, H. Wennerstrom, P. Linse. (1984). Electrical double layer forces: A Monte Carlo study. *Journal of Chemical Physics*, 80, 2221–2228.

F. Helfferich. (1962). *Ion Exchange*, New York: McGraw-Hill.

A.L. Hodgkin, B. Katz. (1949). The effect of sodium ions on the electrical activity of the giant axon of the Squid. *The Journal of Physiology*, 108, 37–77.

M. Homma, Y. Seida, Y. Nakano. (2000). Evaluation of optimum condition for designing high-performance electro-driven polymer hydrogel systems. *Journal of Applied Polymer Science*, 75, 111–118.

Y. Hwang, F. Helfferich. (1987). Generalized model for multispecies ion-exchange kinetics including fast reversible reactions. *Reactive and Functional Polymers*, 5, 237–253.

B.D. Johnson, J.M. Bauer, D.J. Niedermaier, W.C. Crone, D.J. Beebe. (2004a). Experimental techniques for mechanical characterization of hydrogels at the microscale. *Experimental Mechanics*, 44, 21–28.

B.D. Johnson, D.J. Beebe, W.C. Crone. (2004b). Effects of swelling on the mechanical properties of a pH-sensitive hydrogel for use in microfluidic devices. *Materials Science and Engineering C: Biomimetic and Supramolecular Systems*, 24, 575–581.

B.D. Johnson, D.J. Niedermaier, W.C. Crone, J. Moorthy, D.J. Beebe. (2002). Mechanical properties of a pH sensitive hydrogel, *Proceedings of the 2002 Annual Conference of Society for Experimental Mechanics*, Milwaukee, Wisconsin.

A. Katchalsky. (1949). Rapid swelling and deswelling of reversible gels of polymeric acids by ionization. *Experientia*, 5, 319–320.

A. Katchalsky, P.F. Curran. (1965). *Nonequilibrium Thermodynamics in Biophysics*, Massachusetts: Harvard University Press.

M. Kato. (1995). Numerical analysis of the Nernst–Planck–Poisson system . *Journal of Theoretical Biology*, 177, 299–304.

M.G. Kurnikova, R.D. Coalson, P. Graft, A. Nitzan. (1999). A lattice relaxation algorithm for three-dimensional Poisson–Nernst–Planck theory with application to ion transport through the gramicidin a channel. *Biophysical Journal*, 76, 642–656.

W.M. Lai, J.S. Hou, V.C. Mow. (1991). A triphasic theory for the swelling and deformation behaviors of articular cartilage. *ASME Journal of Biomechanical Engineering*, 113, 245–258.

H. Li, T.Y. Ng, J.Q. Cheng, K.Y. Lam. (2003). Hermite-cloud: A novel true meshless method. *Computational Mechanics*, 33, 30–41.

D.R. Lide. (Ed.) (2002). *CRC Handbook of Chemistry and Physics*, 83rd edn. Boca Raton: CRC Press.

A.M. Lowman, N.A. Peppas. (1999). Hydrogels. In: *Encyclopedia of Controlled Drug Delivery*, E. Mathiowitz (Ed.) New York: Wiley, pp. 397–418.

A.D. MacGillivray. (1968). Nernst–Planck equation and the electroneutrality and Donnan equilibrium assumptions. *Journal of Chemical Physics*, 48, 2903–2907.

A.D. MacGillivray, D. Hare. (1969). Applicability of goldman's constant field assumption to biological systems. *Journal of Theoretical Biology*, 25, 113–126.

J. Malmivuo, R. Plonsey. (1995). *Bioelectromagnetism: Principles and Applications of Bioelectric and Biomagnetic Fields*, New York: Oxford University Press.

L.E. Malvern. (1969). *Introduction to the Mechanics of A Continuum Medium*, Englewood Cliffs, New Jersey: Prentice-Hall.

Y. Osada, J.P. Gong. (1993). Stimuli-responsive polymer gels and their application to chemomechanical systems. *Progress in Polymer Science*, 18, 187–226.

W.K. Panofsky, M. Phillips. (1964). *Classical Electricity and Magnetism*, 2nd edn. Reading, Massachusetts: Addison-Wesley.

N.A. Peppas, P. Bures, W. Leobandung, H. Ichikawa. (2000). Hydrogels in pharmaceutical formulations. *European Journal of Pharmaceutics and Biopharmaceutics*, 50, 27–46.

A. Redondo, R. LeSar. (2004). Modelling and simulation of biomaterial. *Annual Review of Materials Research*, 34, 279–314.

J. Ricka, T. Tanaka. (1984). Swelling of ionic gels: Quantitative performance of the Donnan theory. *Macromolecules*, 17, 2916–2921.

B. Roux, T. Allen, S. Berneche, W. Im. (2004). Theoretical and computational models of biological ion channels. *Quarterly Reviews of Biophysics*, 37, 15–103.

I. Rubinstein. (1990). *Electro-Diffusion of Ions SIAM Studies in Applied Mathematics*, Philadelphia: SIAM.

E. Samson, J. Marchand. (1999). Numerical solution of the extended Nernst–Planck model. *Journal of Colloid and Interface Science*, 215, 1–8.

E. Samson, J. Marchand, J.L. Robert, J.P. Bournazel. (1999). Modelling ion diffusion mechanisms in porous media. *International Journal for Numerical Methods in Engineering*, 46, 2043–2060.

S. Selberherr. (1984). *Analysis and Simulation of Semiconductor Devices*, New York: Springer.

M. Shibayama, T. Tanaka. (1993). Volume Phase Transition and Related Phenomena of Polymer Gels. In: *Responsive Gels: Volume Transitions I, Advances in Polymer Science* Vol. 109, K. Dusek (Ed.) Berlin: Springer-Verlag, pp. 1–62.

T. Shiga, Y. Hirose, A. Okada, T. Kurauchi. (1992a). Bending of poly(vinyl alcohol)-poly(sodium acrylate) composite hydrogel in electric fields. *Journal of Applied Polymer Science*, 44, 249–253.

T. Shiga, Y. Hirose, A. Okada, T. Kurauchi. (1992b). Electric field-associated deformation of polyelectrolyte gel near a phrase transition point. *Journal of Applied Polymer Science*, 46, 635–640.

R.A. Siegel. (1990). pH Sensitive Gels: Swelling Equilibria, Kinetics and Applications for Drug Delivery. In: *Pulse and Self-Regulated Drug Delivery*, J. Kost (Ed.) Boca Raton: CRC Press, pp. 129–155.

R.A. Siegel, B.A. Firestone. (1988). pH-dependent equilibrium swelling properties of hydrophobic polyelectrolyte copolymer gels. *Macromolecules*, 21, 3254–3259.

R.A. Siegel, B.A. Firestone, J. Cornejo-Bravo, B. Schwarz. (1991). Hydrophobic Weak Polybasic Gels: Factors Controlling Swelling Equilibrium. In: *Polymer Gels: Fundamental and Biomedical Applications*, D. DeRossi, K. Kajiwara, Y. Osada, A. Yamauchi (Eds.) New York: Plenum Press, pp. 309–317.

R.A. Sjodin. (1971). Ion Transport across Excitable Cell Membranes. In: *Biophysics and Physiology of Excitable Membranes*, W.J. Adelman Jr. (Ed.) New York: Van Nostrand Reinhold Co, pp. 96–124.

A. Syganow, E. von Kitzing. (1999). The drift approximation solves the Poisson, Nernst–Planck, and continuum equation in the limit of large external voltages. *European Biophysics Journal*, 28, 393–414.

T. Tanaka, D. Fillmore, S.T. Sun, I. Nishio, G. Swislow, A. Shah. (1980). Phase transition in ionic gels. *Physical Review Letters*, 45, 1636–1639.

T. Teorell. (1953). Transport processes and electrical phenomena in ionic membranes. *Progress in Biophysics & Molecular Biology*, 3, 305–369.

A. Townshend. Ed. (1995). *Encyclopedia of Analytical Science*, Vol. 1 (A-Che), London: Academic Press.

T. Wallmersperger, B. Kroeplin. (2001). Modelling and Analysis of the Chemistry and Electromechanics. In: *Electroactive Polymer Actuators as Artificial Muscles*, Y. Bar-Cohen (Ed.) SPIE Press, pp. 285–307.

H.H. Woodson, J.R. Melcher. (1968). *Electromechanical Dynamics Part I: Discrete Systems*, New York: John Wiley and Sons.

Q. Yu, J.M. Bauer, J.S. Moore, D.J. Beebe. (2001). Responsive biomimetic hydrogel valve for microfluidics. *Applied Physics Letters*, 78, 2589–2591.

B. Zhao, J.S. Moore. (2001). Fast pH- and ionic strength-responsive hydrogels in microchannels. *Langmuir*, 17, 4758–4763.

http://www.springer.com/978-3-642-02367-5

Smart Hydrogel Modelling

Li, H.

2009, XVII, 359 p., Hardcover
ISBN: 978-3-642-02367-5